FEATURE ARTICLE

Conical Intersections: The New Conventional Wisdom

David R. Yarkony

Department of Chemistry, Johns Hopkins University, Baltimore, Maryland 21218

Received: October 11, 2000; In Final Form: February 23, 2001

During the past decade the perception of conical intersections has changed. It is now appreciated that what was once viewed largely as a theoretical curiosity is an essential aspect of electronically nonadiabatic processes. Concomitantly, our understanding of this singular consequence of the Born−Oppenheimer separation of nuclear and electronic motion has grown enormously. In this work the theory of conical intersections is reviewed.

I. Introduction

While the adiabatic or Born−Oppeneimer single potential energy surface approximation is valid for the preponderance of chemical processes, nonadiabatic transitions, which extend nuclear motion to more than one Born−Oppenheimer potential energy surface, are at the heart of such essential processes as vision, light harvesting,[1,2] charge transfer reactions,[3] and a myriad of processes in the upper atmosphere. In the past decade it has become apparent that conical intersections, including those of two states of the same symmetry, which were once little more than a theoretical curiosity, are an essential aspect of electronically nonadiabatic phenomena, touching most if not all areas of nonadiabatic chemistry. From the energy storage initiated by the cis−trans isomerization of retinal protonated Schiff base in bacteriorhodopsin,[49] to the observation of quantized or steplike structure in the rate constant for photodissociation of ketene,[50,51] to ultrafast decay of azulene,[30] to the geometric phase in $H + H_2$ scattering,[48,52] conical intersections must be considered.

Consequently there has been considerable interest in nonadiabatic processes induced by conical interactions.[4−22] Conical interactions influence nonadiabatic processes in several ways. The interstate couplings are large near, and singular at, a conical intersection. These large couplings can lead to ultrafast decay of electronically excited states; that is, they facilitate upper state to lower state (UtL) transitions.[15,23−31] Conical intersections with the appropriate topography can also facilitate transitions from a lower state to an upper state (LtU),[32,33] for example, in endothermic charge-transfer reactions,[34] a point that has received inadequate attention. A wave packet passing through a conical intersection, as opposed to a transition state, may be routed to more than one product.[35,36] Finally, conical intersections give rise to the geometric phase effect,[37−39] which necessitates changes in the nuclear Schrödinger equation in the adiabatic representation.

In this work recent advances in our understanding of this consequence of the Born−Oppenheimer[40] separation of nuclear and electronic motion are reviewed. Whenever possible, the basic ideas are illustrated with examples. However, since much of the progress in the past decade has been a consequence of formal and algorithmic advances, for those interested in a more complete description, additional details are provided. Thus, section II provides an introduction to the electronic structure topics to be developed in this review while section III describes those topics in more detail. In these sections conical intersections are defined, and such essential concepts as the $g-h$[41] or branching[32] plane, the geometric phase effect,[37,39,42] the noncrossing rule,[43] the derivative couplings,[44] and diabatic bases[45,46] are reviewed. The effects of the spin−orbit interaction on the geometric phase effect and the noncrossing rule are discussed. The spin−orbit interaction is singled out for special consideration since it produces qualitative changes in the locus of points conical intersection. While all conical intersections produce the geometric phase effect, not all conical intersections are topographically equivalent. In section IV the time dependent Schrödinger equation is used to consider the effect of the topography of a conical intersection on nuclear dynamics. As a prelude to this treatment, section III includes a perturbative[38,47] analysis of the energetics and derivative couplings near a conical intersection. The preponderance of fully quantum mechanical treatments of nonadiabatic nuclear dynamics near conical intersections[4−9,11,12,14−22] are carried out in a diabatic basis[15] to avoid numerical problems associated with the singular derivative couplings in the adiabatic representation.[48] However, here the adiabatic representation is used. It has been argued that in the appropriate coordinates, the singularity in the derivative coupling at the conical intersection is quite tractable and can in fact be used to advantage.[33] Section V describes some open questions raised in this work, while section VI briefly considers directions for future investigation.

The focus of this overview is the conical intersection itself. Therefore, there is no separate examples/applications section. Rather, conical intersections determined as part as of larger studies are included in the individual sections as illustrations. The illustrations are drawn from two studies ongoing in my laboratory, the dissociation of photoexcited HNCO,

$$\mathrm{HNCO}(S_0 = X^1A') + h\nu \rightarrow$$
$$\mathrm{HNCO}(S_1 = {}^1A'') \rightarrow H + \mathrm{NCO}(X^2\Pi) \quad (1a)$$
$$\rightarrow \mathrm{HN}(a^1\Delta) + \mathrm{CO} \quad (1b)$$

which has been the object of many experimental and theoretical

10.1021/jp003731u CCC: $20.00
Published on Web 06/12/2001

studies,[53−56] and the highly nonadiabatic reaction of oxygen and water,

$$O(^3P) + H_2O \rightarrow OH(X^2\Pi) + OH(A^2\Sigma^+) \qquad (2)$$

where the reactants are in any of the $1^3A'$, $1,2^3A''$ states while the products are in either the $3^3A'$ or $3^3A''$ states.

In HNCO photodissociation a large barrier precludes directed dissociation on S_1 to produce H + NCO.[57,58] Access to this channel is achieved via S_1-S_0 internal conversion facilitated by a seam of conical intersection. The seam was determined as a function of R(C−N), reflecting the fact that following photoexcitation R(C−N) increases as a consequence of a stable trans isomer on S_1.[59] These conical intersections are considered in this work. The $O + H_2O \rightarrow OH(X^2\Pi) + OH(A^2\Sigma^+)$ reaction is key to understanding the ultraviolet plume originating from the control engines of the space shuttle or the Soyez engines of Russian service vehicles.[60−62] A proposed mechanism reflects insights gained from points on a portion of the seam conical intersection. The HOH−O conical intersection considered in this review is essentially collinear. This seam of conical intersection can be understood as the well-known[63,64] $^1\Sigma^+-^1\Pi$ seam of conical intersection in water, coupled to an $O(^3P)$ in a $^3\Pi$ orientation relative to the HOH axis. This high-symmetry arrangement of the nuclei, which is accessible to both the reactants and products with little or no barrier (beyond the endoergicity), provides a favorable path for reaction 2.

II. Overview

Within the Born−Oppenheimer separation of nuclear and electronic motion the Born−Oppenheimer potential energy surfaces, $E_I^{0,a}(\boldsymbol{\tau})$, and the adiabatic electronic states $\Psi_I^{0,a}(\mathbf{r};\mathbf{R})$ are the eigenvalues and eigenfunctions of the electronic Hamiltonian $\mathbf{H}^{el,0}(\mathbf{r};\mathbf{R})$. Here $\mathbf{r} = (\mathbf{r}_1, \mathbf{r}_2, ..., \mathbf{r}_{N^{el}})$ are the coordinates of the N^{el} electrons, $\mathbf{R} = (\mathbf{R}_1, \mathbf{R}_2, ..., \mathbf{R}_{N^{nuc}})$ are the space-fixed frame coordinates of the N^{nuc} nuclei, and we have noted that the $E_I^{0,a}$ depend only on $\boldsymbol{\tau}$, the $3N^{nuc} - 6 = N^{int}$ internal coordinates, defined below.

A. Conical Intersections and the $g-h$ Plane: Privileged Directions. At $\boldsymbol{\tau}_x$ (or $\mathbf{R}_x$), a point of conical intersection, two Born−Oppenheimer potential energy surfaces, denoted I and $J = I + 1$, intersect forming a double cone. The *seam* is the locus of these points of conical intersection. The dimension of the seam is discussed below. A seam of conical intersection is pictured in Figure 1 from two perspectives. While neither part is complete, taken together they correctly describe the seam. Figure 1a depicts a single point on the seam, $\boldsymbol{\tau}_x$. The adiabatic energies, $E_K^{0,a}$, $K = I, J$, are plotted vs the two internal coordinates, denoted $\mathbf{g}^{IJ}$ (the tuning coordinate[65]) and $\mathbf{h}^{IJ}$ (the coupling coordinate), for which the energy has the shape of a double cone. Here "tuning" refers to the fact that one can "tune in" on a specific conical intersection by changing the displacement along $\mathbf{g}^{IJ}$. Figure 1b depicts the connectivity of the points of conical intersection, the seam. In that figure the $E_K^{0,a}$, $K = I, J$, are plotted against one conical (a coupling ($\mathbf{h}^{IJ}$) *or* tuning ($\mathbf{g}^{IJ}$)) coordinate (here $\mathbf{g}^{IJ}$ is used) and one nonconical or seam (z) coordinate. In Figure 1b the seam is a (thick dashed) line and the topography of the lower (upper) potential energy surface along the seam is that of a (an upside down) ridge. This plot, while accurate, is in a sense misleading. It leaves the impression that if the seam were a convex up parabola, the extreme point would resemble a transition state, with the $\mathbf{g}^{IJ}$ direction playing the role of the reaction coordinate. This is not the case. The second conical direction evident in Figure 1a makes the topography of the lower surface more like that of series of extrema with two negative eigenvalues. This analogy to extrema

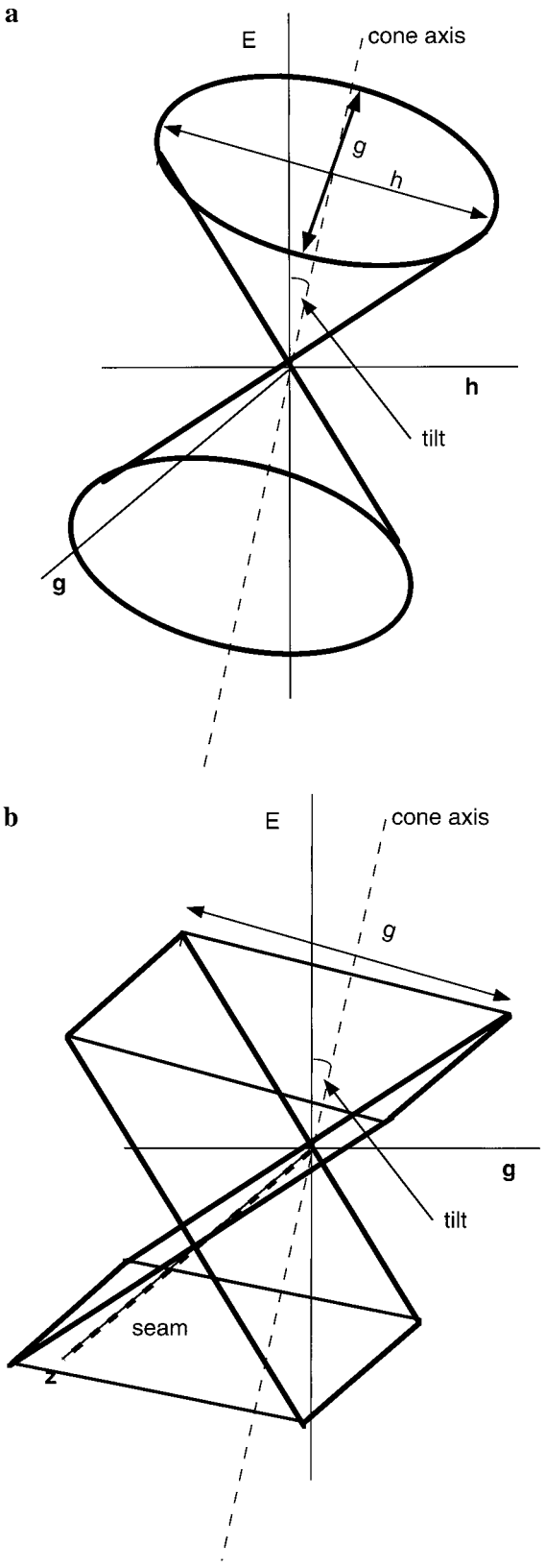

Figure 1. (a) Tilted asymmetric conical intersection. $E_I^{0,a}$, lower cone, and $E_J^{0,a}$, upper cone, plotted in the branching or $g-h$ plane. (b) Conical intersection in (a) plotted against one coordinate in the $g-h$ plane and one coordinate on the seam perpendicular to the $g-h$ -plane. $E_I^{0,a}$, lower wedge, and $E_J^{0,a}$, upper wedge. The point of conical intersection in (a) becomes the ridge line in (b).

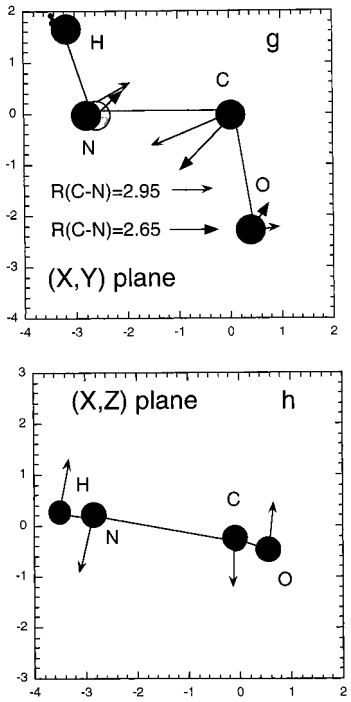

Figure 2. Branching, or $g-h$, plane. $\mathbf{g}^{IJ}$ (top panel) and $\mathbf{h}^{IJ}$ (bottom panel) in terms of atom-centered displacements for HNCO with $R(\mathrm{C-N}) = 2.95a_0$, where the remaining parameters are chosen to minimize the energy of the point of intersection. Also shown in the top panel is $\mathbf{g}^{IJ}$ with $R(\mathrm{C-N}) = 2.65a_0$.

is only approximate since $E_I^{0,a}$ is not differentiable at $\boldsymbol{\tau}_x$. In summary, the minimal description of the energetics of a seam of conical intersection requires at least four dimensions, E, $\mathbf{g}^{IJ}$ *and* $\mathbf{h}^{IJ}$, and one seam coordinate. In this case the ridge pictured in Figure 1b becomes a "ridge" of mountain peaks.

$\mathbf{g}^{IJ}$ and $\mathbf{h}^{IJ}$ are nuclear displacements akin to the normal modes characteristic of an equilibrium geometry. The plane formed by these two coordinates, the branching[32] or $g-h$[41] plane, is a key concept in the theory of conical intersections. Its determination is an essential first step in characterizing a conical intersection. As discussed in section IIIa $\mathbf{g}^{IJ}$ is the gradient of the energy difference while $\mathbf{h}^{IJ}$ is, to a good approximation, the product of the energy difference and the derivative coupling vector; see below. Figure 2 depicts the two displacements defining the $g-h$ plane in terms of atom-centered displacements for a point on the $S_1(^1A'')-S_0(X^1A')$ seam of conical intersection in HNCO.

B. Noncrossing Rule. The dimensionality of the seam of conical intersection is described by the noncrossing rule, deduced by Wigner and von Neumann[43] some 70 years ago. While generally applicable, this rule is most relevant to conical intersections where symmetry does not play a role, that is, conical intersections of two states of the same symmetry, or just same-symmetry intersections. According to this *noncrossing rule the seam of conical intersection* (for $\mathbf{H}^{\mathrm{el},0}$ the usual Coulombic Hamiltonian) *may have dimension* $N^{int} - 2$*, for same-symmetry intersections where* N^{int} *is the number of internal degrees of freedom.* Equivalently, *two internal coordinates must be varied to find an intersection*.

This result is perhaps counterintuitive. Consider a model two electronic state problem:

$$\mathbf{H}^{\mathrm{el},0}(\boldsymbol{\tau}) = \begin{pmatrix} E_1^{0,a}(\boldsymbol{\tau}) & 0 \\ 0 & E_2^{0,a}(\boldsymbol{\tau}) \end{pmatrix}$$

We seek the $\boldsymbol{\tau} = \boldsymbol{\tau}_x$, for which $E_1^{0,a}(\boldsymbol{\tau}_x) - E_2^{0,a}(\boldsymbol{\tau}_x) = 0$. Since this is one equation, its solution may be achieved by varying one internal coordinate, for any choice of the remaining $N^{\mathrm{int}} - 1$ internal coordinates. Of course, solutions may not exist for real values of the coordinates, so we would say the seam *may* have dimension $N^{\mathrm{int}} - 1$ or that the solution space has codimension 1. However, even with this caveat the result is NOT correct. The problem with this argument is that it assumes that the $E_I^{0,a}$ are independent functions of $\boldsymbol{\tau}$. They are not, in general, since they are the eigenvalues of a single matrix. When $E_1^{0,a}(\boldsymbol{\tau})$ and $E_2^{0,a}(\boldsymbol{\tau})$ come from distinct symmetry blocks, they are independent functions of $\boldsymbol{\tau}$ and $N-1$ is, in fact, the correct answer. However, in that case N is the number of internal degrees of freedom, consistent with the symmetry in question.

Thus, the noncrossing rule describes what can be, rather than what is. It is not an existence theorem. Its implication, that two internal coordinates must be varied to find an intersection, if it exists, is not a practical means of locating points on the seam. Perhaps for this reason, as recently as the 1970s, the importance and even the existence of conical intersection of two states of the same symmetry were questioned.[66,67] In section III we revisit the original work of von Neumann and Wigner while discussing a practical approach for locating conical intersections.[68]

C. Derivative Couplings and the Adiabatic and Diabatic Representations. Since the locus of points of conical intersection is a space of dimension $N^{\mathrm{int}} - 2$ one might question the importance of this topographical feature since it occupies a negligible volume in nuclear coordinate space. In fact, conical intersections would be of limited importance if it were not for the derivative couplings, projected gradients of the electronic wave functions

$$f_{W_i}^{JI}(\boldsymbol{\tau}) = \left\langle \Psi_J^{0,a}(\mathbf{r};\mathbf{R}) \middle| \frac{\partial}{\partial W_i} \Psi_I^{0,a}(\mathbf{r};\mathbf{R}) \right\rangle_{\mathbf{r}}$$

These interactions provide the coupling between the adiabatic electronic states. It is the finite range of these coupling that extends the "effective size" of the conical intersections to a nonnegligible volume and thus are responsible for nonadiabatic events.

In the definition above W_i is a nuclear coordinate. While the gradient of the $E_K^{0,a}$ with respect to noninternal coordinates vanishes, as a result of the $\mathbf{R}$ dependence of $\Psi^{0,a}$, the derivative couplings are nonzero for W_i, an internal or noninternal coordinate. Derivative couplings with respect to internal coordinates are of principal concern in this review. However, the derivative couplings with respect to noninternal coordinates have observable consequences giving rise to λ-doubling in diatomic molecules.[69] Other consequences of this class of derivative couplings are described in section III.

While of fundamental importance the derivative couplings are frequently cited as difficult to evaluate,[48] being singular, in the adiabatic representation, at a point of conical intersection. This has limited the use of the adiabatic representation for the description of nonadiabatic dynamics and led to the development of the *diabatic electronic states*.[45,46,70,71] For a historical perspective on diabatic states including reference to the early work of Lichten,[72] O'Malley,[73] and Smith,[70] see ref 71. Diabatic states, constructed from the adiabatic states to preserve the concept of an electronic energy, are designed to reduce or eliminate the derivative coupling.[45,74]

Because of the computational problems caused by the singularity in the derivative coupling, its removal is a key issue in studying nuclear dynamics near conical intersections.[75]

Surprisingly, perhaps, the singularity is comparatively easy to remove. In section III we describe the nature of the singularity in the derivative coupling and how it can be eliminated by a transformation to approximate or quasi-diabatic states. Two approaches are described, quasi-diabatic states based on a perturbative determination of the derivative coupling[47] and on smoothness of a molecular property.[76−78] Using (ρ, ϕ), polar coordinates in the $g-h$ plane, we show (section IIIA) that the singular part of the derivative coupling is given by

$$(1/\rho)f_{\phi}^{JI} = \frac{1}{2\rho}\frac{\partial}{\partial\phi}\lambda(\phi) \xrightarrow{g/h\to 1} \frac{1}{2\rho}$$

where $\lambda(\phi)$ is expressed in terms of g and h, the lengths of the vectors defining the $g-h$ plane. It has the above indicated particularly simple form when $g/h = 1$ (identified below as a Jahn−Teller,[79,80] vertical symmetric or peaked, cone). We further demonstrate (see, for example, Figure 7 in section III) that *this approximation is of sufficient quality to obviate the need to determine this largest component of the derivative coupling using ab initio wave functions*. It is then shown that the rotation of the pair of adiabatic states by $-\lambda(\phi)/2$ produces a pair of approximate diabatic states with a nonsingular derivative coupling.

Although diabatic bases are used for the preponderance of the fully quantum mechanical treatments of nonadiabatic dynamics involving conical intersections, recent work suggests that the adiabatic representation, which offers conceptual advantages,[5] may not be as intractable as previously suggested.[33] The point is discussed in section V.

D. Complex-Valued Hamiltonians and the Spin−Orbit Effect. The preponderance of this presentation considers the nonrelativistic (Coulomb) Hamiltonian, which is real-valued. The noncrossing rule stated above applies to this real-valued (symmetric) Hamiltonian. However, when the number of electrons is odd, relativistic effects, in particular the inclusion of the spin−orbit interaction,[81,82] lead to a complex-valued, hermitian, Hamiltonian.

For a complex-valued Hamiltonian the conclusion of the noncrossing rule is that the dimensionality of the seam is $N^{\text{int}} - 3$. The $N^{\text{int}} - 3$ result is, in turn, rigorous for the Hamiltonian considered, that is, a Hamiltonian with a single degeneracy. However, for an odd number of electrons there is an additional complicating factor, Kramers' degeneracy.[83] Kramers' degeneracy, a consequence of time reversal symmetry,[84] requires states of systems with odd numbers of electrons to be (at least) 2-fold degenerate. This changes the nature of the Hamiltonian that must be considered when looking for intersecting surfaces.[85] When C_s symmetry can be imposed, the result remains $N^{C_s} - 3$. Here, N^{C_s} is the number of degrees of freedom that preserve C_s symmetry. However, in the absence of symmetry, the seam, if it exists, has dimension $N^{\text{int}} - 5$.[85]

This change in dimensionality to $N^{C_s} - 3$ or N^{int}-− 5 has profound implications for the geometric phase effect discussed below. These implications are illustrated using a molecule in a doublet state constrained to C_s symmetry. We consider the intersection of two adiabatic eigenstates of the nonrelativistic Hamiltonian, perturbed by the spin−orbit interaction. As described in section III, the Hamiltonian matrix has the form

$$\begin{bmatrix} E_I^{0,a} & i\gamma \\ -i\gamma & E_J^{0,a} \end{bmatrix}$$

where γ is real. *This Hamiltonian has a seam of conical intersection of dimension* $N^{\text{int}} - 3$ *comprising the subspace of the nonrelativistic seam for which the spin−orbit coupling vanishes.* For a triatomic molecule the intersection seam reduces to a point, as is illustrated in Figure 3.

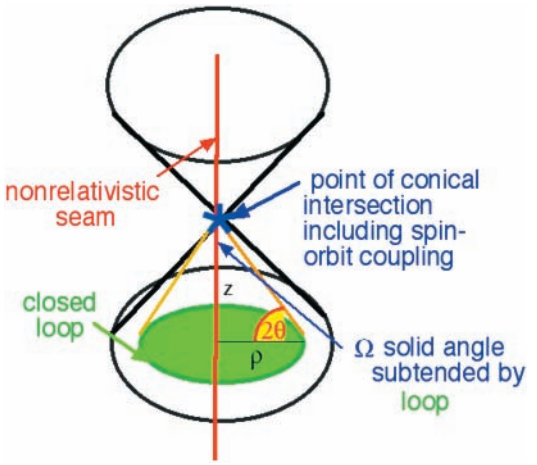

Figure 3. $^2A_1 - {}^2B_2$ conical intersection seam without spin−orbit interaction, s_0 (red) and with spin−orbit interaction, s_1 (purple point). Also shown is a closed loop (green) surrounding s_0 subtending a solid angle Ω with respect to the single conical intersection point, s_1.

E. Geometric Phase Effect. *(i) Diabolical Conical Intersections.* Longuet−Higgins[37] noted that when a real-valued adiabatic wave function is transported around a *closed* loop in nuclear coordinate space containing a conical intersection the wave function must change sign. This is the geometric phase effect. The geometric phase effect, perhaps the signature property of a conical intersection, necessitates modification of the nuclear Schrödinger equation built from adiabatic electronic states.[37,42] See section IV. It is notable for its long range, affecting nuclear dynamics under conditions when the wave function never encounters the associated conical intersection.[52,86] When the conical intersections in question arise from two states of the same symmetry, they are difficult to anticipate and may go unnoticed. For that reason we have, following Berry,[87] termed such conical intersections, *diabolical*.[41,88]

(ii) Proving the Existence of a Conical Intersection. Conical intersections determined from numerical procedures are never exactly degenerate. The verification of the geometric phase effect, however, provides incontrovertible evidence of the existence of a conical intersection. This approach has been used in the past to establish the existence of conical intersections.[89−91] An alternative, much less tedious, method for confirming the existence of a point of conical intersection, evaluates the circulation, the line integral[92] around a closed loop, of the derivative coupling.[47] It has been shown[47] that *if the loop contains a conical intersection, then as the radius approaches zero*

$$\oint \mathbf{f}^{JI}(\boldsymbol{r})\cdot d\boldsymbol{r} \to \pi$$

On the other hand, if the closed loop does not enclose a conical intersection, the $\rho \to 0$ limit of the circulation is 0.[42] In the language of the geometric phase effect, *for an infinitesimal loop the circulation of the derivative coupling equals the accumulated phase.* Numerous applications of this approach have been reported.[51,93−96]

To use the above results, loops in nuclear coordinate space containing a conical intersection are required. Such loops are readily defined using the $\mathbf{g}^{IJ}$ and $\mathbf{h}^{IJ}$ vectors. Figure 4 displays the nuclear configurations that constitute a loop around the

CHART 1

parameters	classification[33]	classification[32]
$\Delta_{gh} = s^x = s^y = 0$	vertical symmetric	peaked
$\Delta_{gh} \neq 0$, $s^x = s^y = 0$	vertical asymmetric	
$\Delta_{gh} = 0$, s^x and/or $s^y \neq 0$	tilted symmetric	~semilevel ($s^x/d_{gh} = s^y/d_{gh} \sim 1$) ~sloped ($s^x/d_{gh} = s^y/d_{gh} < 1$)

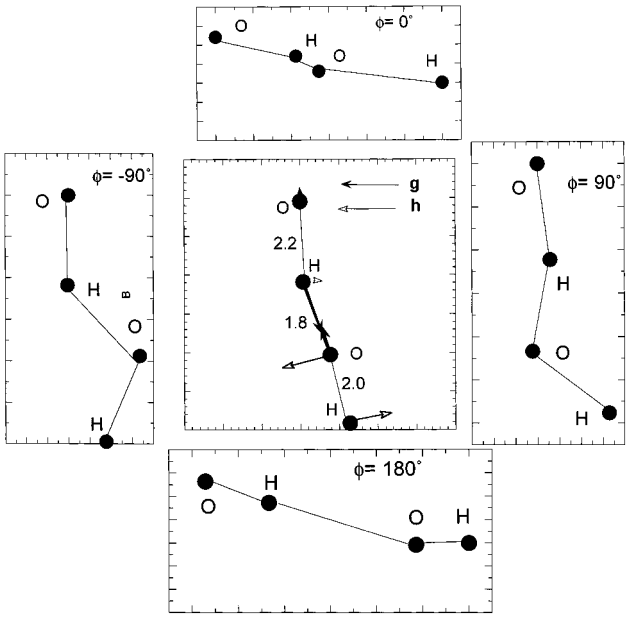

Figure 4. For $O(^3P) + H_2O$: Center figure gives $g-h$ or branching space for a point on the $2^3A''-3^3A''$ seam of conical intersection. Outer figures describe a loop around that point of conical intersection. $\phi = 0, \pi$ correspond to $+x$, $-x$ axis displacements, while $\phi = \pi/2, -\pi/2$ correspond to $+y$, $-y$ axis displacements.

(nearly) collinear conical intersections in O−HOH noted in the Introduction. It is also worth noting that the potential for bifurcating nuclear dynamics exists. Motion along the positive $\mathbf{g}^{IJ}$ direction points toward $H_2O + O$, which motion along the $\pm\mathbf{h}^{IJ}$ axis points toward OH + OH.

(iii) Spin−Orbit Interaction and the Geometric Phase Effect. The affect of the spin−orbit interaction on the geometric phase effect in odd electron systems is particularly interesting. Since the dimension of the seam is now no bigger than $N^{\text{int}} - 3$, the idea of a loop enclosing or not enclosing a conical intersection must be revised.[39] As illustrated in Figure 3, one should consider the solid angle, Ω, subtended by the loop viewed from the point of conical intersection. Berry has shown[39] that the change in phase of the wave function is $\exp(\pm i\Omega/2)$, which becomes -1 ($\Omega = 2\pi$) when the loop contains the point of intersection. Here the $-$ (+) sign applies to the lower (upper) state. An example of these ideas, suggested by the work of Stone[97] (see also ref 98), will be provided in sections IIIE and IIIF. It is also shown that in the case of a complex hermitian Hamiltonian the circulation of the derivative coupling does not equal the accumulated phase.

F. Conical Topographies and Elementary Cones. In the adiabatic representation nonadiabatic transitions are driven by the derivative coupling. At the conical intersection the derivative coupling is singular. To quantify the propensity for a nonadiabatic transition near a conical intersection, requires, at minimum, the energy and singular part of the derivative couplings. Using perturbation theory, one can show that the conical topography is completely described by nuclear displacements in the branching[32] or $g-h$[41] plane defined by the tuning and coupling coordinates $\mathbf{g}^{IJ}$ and $\mathbf{h}^{IJ}$. In this $g-h$ plane the conical topography can be described, in terms of four conical parameters, g, h, s_x, and s_y deduced from the characteristic vectors $\mathbf{g}^{IJ}$, $\mathbf{h}^{IJ}$, and $\mathbf{s}^{IJ}$ (the gradient of $(E_I^{0,a} + E_J^{0,a})/2$ see below). In particular, it is shown[41] that $E_K^{0,a}$ is given by

$$\mathbf{E}^{0,a}(\rho,\phi) \approx \rho[(s_x \cos\phi + s_y \sin\phi)\mathbf{I} - (g^2\cos^2\phi + h^2\sin^2\phi)^{1/2}\boldsymbol{\sigma}_z]$$

where $\boldsymbol{\sigma}_w$ ($w = x, y, z$) are the Pauli spin matrices,[84] $\mathbf{I}$ is a 2×2 unit matrix and $\rho = 0$ is a point of conical intersection. In section III we demonstrate (see, for example, Figure 7 in that section) that *this approximation is of sufficient quality to obviate the need to determine the electronic energy using an ab initio wave function in the immediate vicinity of a conical intersection*.

It will prove useful re-express the conical parameters as, a strength parameter, $d_{gh}^2 = g^2 + h^2$, an asymmetry parameter, $\Delta_{gh} = (g^2 - h^2)/(g^2 + h^2)$, and two tilt parameters, $s^x/d_{gh} = s_x/g$ and $s^y/d_{gh} = s_y/h$. This parametrization (see eqs 16 and 17 in section IIIC) and an analysis of the nuclear Schrödinger equation near a conical intersection, described in section IV, suggest that it is useful to classify the double cones as in Chart 1. Here the attribute "symmetric" refers only to Δ_{gh}, the middle column gives the labeling used herein, and the third column indicates approximate correspondences with an earlier labeling due to Ruedenberg and co-workers.[32] These basic cones are pictured in Figure 5. Here the vertical symmetric double cone is that corresponding to a symmetry-required E-type C_{3v} irreducible representation.[79] Only this double cone, for which $g = h$ and $s_x = s_y = 0$, is fully symmetric; that is, the energies are independent of ϕ, the angle that takes you around the cone. Note too the striking difference in the ϕ dependence induced by $\Delta_{gh} \neq 0$, middle panels, and by $s_x \neq 0$ and $\neq s_y$, bottom panels. The implications of this difference are discussed in section IV using wave packet dynamics.

III. Conical Intersections: In More Detail

The adiabatic electronic potential energy surfaces, $E_I^{0,a}(\boldsymbol{\tau})$, are the eigenvalues of $\mathbf{H}^{\text{el},0}$, the nonrelativistic coulomb Hamiltonian:

$$[H^{\text{el},0}(\mathbf{r};\mathbf{R}) - E_I^{0,a}(\boldsymbol{\tau})]\Psi_I^{0,a}(\mathbf{r};\mathbf{R}) = 0 \qquad (3)$$

We will also have occasion to consider $\mathbf{H}^{\text{el}} = \mathbf{H}^{\text{el},0} + \mathbf{H}^{\text{so}}$, where $\mathbf{H}^{\text{so}}$ is the spin−orbit operator treated at the Breit-Pauli level.[81,82,99] However, even in this case, for molecules comprised of low Z ($\leq\sim$36) atoms, it is, as discussed below, useful to consider adiabatic states described by eq 3.

When only $\mathbf{H}^{\text{el},0}$ is considered, $\boldsymbol{\tau}_x$, points of conical intersection of states I and $J = I + 1$, are a subset of the internal coordinates $\boldsymbol{\tau}$, for which $\Delta E_{IJ}^{0,a}(\boldsymbol{\tau}) \equiv E_I^{0,a}(\boldsymbol{\tau}) - E_J^{0,a}(\boldsymbol{\tau}) = 0$. When $\mathbf{H}^{\text{so}}$ is included, degenerate states of $\mathbf{H}^{\text{el}}$ in the adiabatic basis $\Psi_I^{0,a}$ are sought.

A. $g-h$ or Branching Plane. The vectors $\mathbf{g}^{IJ}$ and $\mathbf{h}^{IJ}$, rigorously defined below, form the basis of a generalized polar coordinate system, the intersection adapted,[32] or conical,[41]

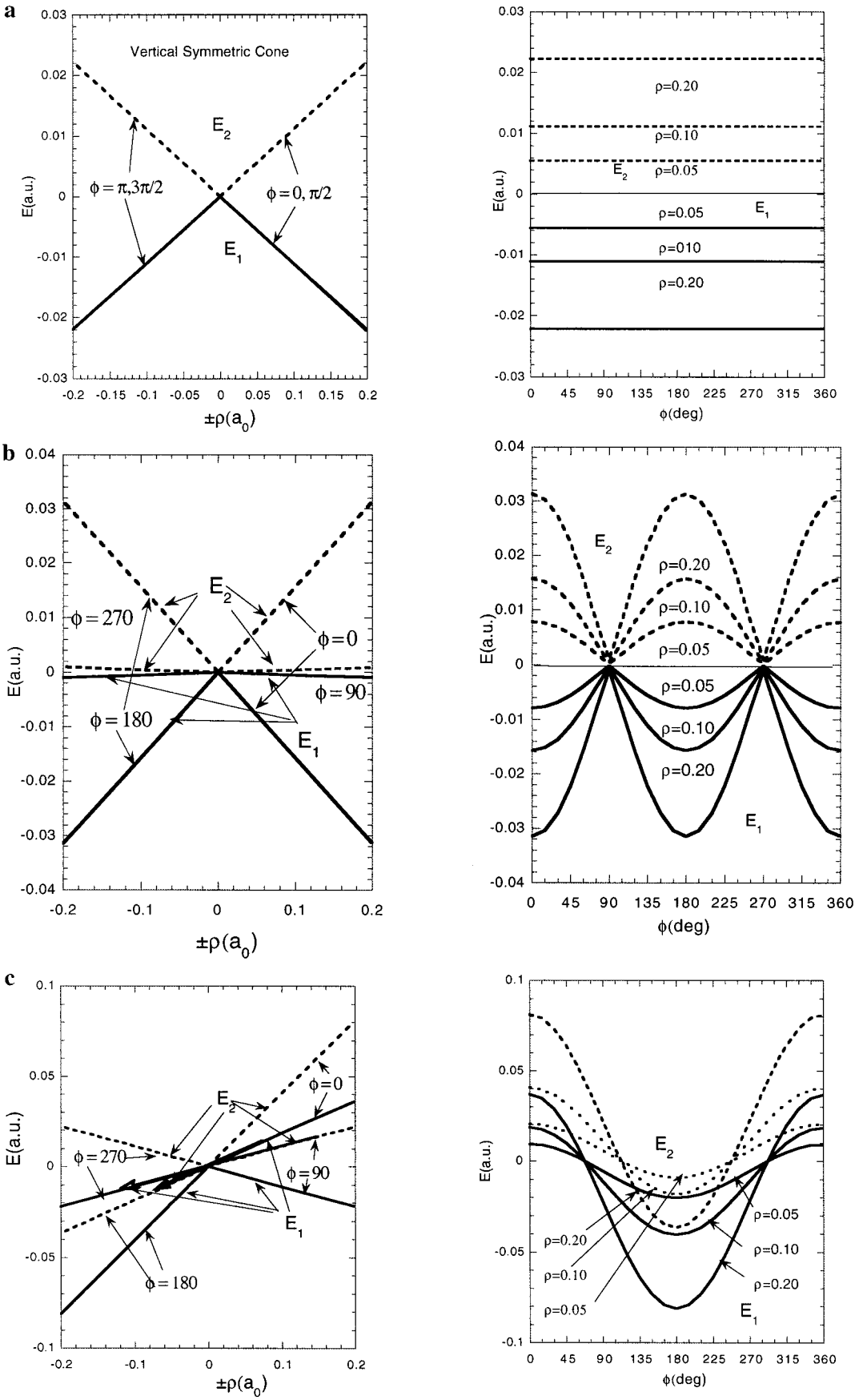

Figure 5. Sections of the potential energy surface for (a) a vertical symmetrical cone (top panel), $d_{gh} = 0.11$ and $\Delta_{gh} = s_x = s_y = 0$; (b) vertical asymmetric cone, $d_{gh} = 0.11$, $\Delta_{gh} = 0.99$, and $s_x = s_y = 0$ (middle panel); and (c) tilted symmetric cone (bottom panel) $d_{gh} = 0.11$, $\Delta_{gh} = 0$, $s_x = 0.2$ and $s_y = 0$. Dashed (solid) lines are upper (lower) cone.

cooordinates where $\mathbf{x} = \mathbf{g}^{IJ}/g$, $\mathbf{y} = \mathbf{h}^{IJ}/h$, $||\mathbf{g}^{IJ}|| = g$, $||\mathbf{h}^{IJ}|| = h$. The remaining $N^{\text{int}} - 2$ internal coordinates, referred to as seam coordinates, and denoted $\mathbf{z}^i$, $i = 1, ..., N^{\text{int}} - 2$ are orthogonal to the (x, y) plane and to each other. A seam coordinate $\mathbf{z}^3$ for

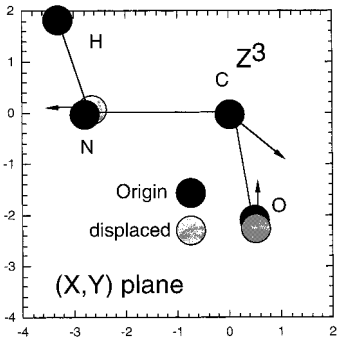

Figure 6. For HNCO: seam coordinate $z^{(3)}$ for the conical intersection point in Figure 2 and displacement along the seam coordinate to an adjacent point of conical intersection.

the $g-h$ plane in Figure 2 is given in Figure 6 which also illustrates the result of a displacement along $-\mathbf{z}^3$. This displacement, orthogonal to the $g-h$ plane, approximately connects two points on the seam of conical intersection, $R(\mathrm{C-N}) = 2.65a_0$ and $R(\mathrm{C-N}) = 2.95a_0$. The displaced point is only on the seam in an approximate sense since orientation of the $g-h$ plane changes with the position on the seam; that is, the seam is not a (generalized) straight line.

For motion in the $g-h$ plane it is useful to define the polar coordinates, ρ a size coordinate, and ϕ a shape coordinate by $x = \rho \cos \phi$, $y = \rho \sin \phi$. For fixed ρ, the path mapped out by increasing ϕ by 2π represents a circle surrounding the point of conical intersection. For this reason these polar coordinates are useful in the description of geometric phase effect. An example of motion for ρ fixed and $0 < \phi < 2\pi$ is shown in Figure 4. See also ref 101.

(i) Evaluation of g^{IJ} and h^{IJ}. In the past, the $g-h$ plane was determined by fitting the energies along loops around the conical intersection. However, with the use of analytic gradient techniques[44] determination of the $g-h$ plane is no harder than determination of the gradient of the adiabatic energy,[102,103] $\nabla E_J^{0,a}(\boldsymbol{\tau})$. Below is outlined the basic idea behind this important advance.[47]

Expand $\Psi_K^{0,a}$ in a configuration state function[104] (CSF, ψ) basis:

$$\Psi_K^{0,a}(\mathbf{r};\mathbf{R}) = \sum_{\alpha=1}^{N^{CSF}} c_\alpha^K(\boldsymbol{\tau})\, \psi_\alpha(\mathbf{r};\mathbf{R}) \tag{4a}$$

where the $\mathbf{c}^K$ are solutions of the configuration interaction problem:

$$[\mathbf{H}^{el,0}(\boldsymbol{\tau}) - E_K^{0,a}(\boldsymbol{\tau})]\mathbf{c}^K(\boldsymbol{\tau}) = 0 \tag{4b}$$

and $\mathbf{H}^{el,0}(\boldsymbol{\tau})$ is the electronic Hamiltonian in the ψ basis. Then ($\mathbf{g}^{IJ}$, $\mathbf{h}^{IJ}$) are given by

$$2\mathbf{g}^{IJ}(\boldsymbol{\tau}) = \mathbf{c}^{I\dagger}(\boldsymbol{\tau}_x)[\nabla\mathbf{H}^{el,0}(\boldsymbol{\tau})]\mathbf{c}^I(\boldsymbol{\tau}_x) - \mathbf{c}^{J\dagger}(\boldsymbol{\tau}_x)[\nabla\mathbf{H}^{el,0}(\boldsymbol{\tau})]\mathbf{c}^J(\boldsymbol{\tau}_x) \tag{5a}$$

$$\mathbf{h}^{IJ}(\boldsymbol{\tau}) = \mathbf{c}^{I\dagger}(\boldsymbol{\tau}_x)[\nabla\mathbf{H}^{el,0}(\boldsymbol{\tau})]\mathbf{c}^J(\boldsymbol{\tau}_x) \tag{5b}$$

It is also convenient to define

$$2\mathbf{s}^{IJ}(\boldsymbol{\tau}) = \mathbf{c}^{I\dagger}(\boldsymbol{\tau}_x)[\nabla\mathbf{H}^{el,0}(\boldsymbol{\tau})]\mathbf{c}^I(\boldsymbol{\tau}_x) + \mathbf{c}^{J\dagger}(\boldsymbol{\tau}_x)[\nabla_{\boldsymbol{\tau}}\mathbf{H}^{el,0}(\boldsymbol{\tau})]\mathbf{c}^J(\boldsymbol{\tau}_x) \tag{5c}$$

In eqs 5a−c, $\nabla\mathbf{H}^{el,0}$, the gradient of the Hamiltonian matrix, is the same gradient used to evaluate $\nabla E_J^{0,a}$. This enables $\mathbf{g}^{IJ}$, $\mathbf{h}^{IJ}$, $\mathbf{s}^{IJ}$, and $\mathbf{f}^{IJ}$ (see below) to be evaluated with a single algorithm.[44] Construction of $\nabla\mathbf{H}^{el,0}$ and the evaluation of the right-hand sides of eqs 5a−5c are described in refs 44 and 68.

(ii) Symmetry and the Orthogonality of $\mathbf{g}^{IJ}$ and $\mathbf{h}^{IJ}$. Symmetry is an important aspect of the $g-h$ plane. Figure 2 depicted the two coordinates defining the $g-h$ plane in terms of atom-centered displacements. There the role of symmetry is evident. The molecule is (approximately) in the $X-Y$ plane in nuclear coordinate space. The states in question, the S_0 and S_1 states of HNCO, have ^{1}A′ and ^{1}A″ symmetry. The mode labeled $\mathbf{h}^{IJ}$, the coupling mode, is seen to have the a″ symmetry required to couple an A′ and an A″ state. The tuning mode, $\mathbf{g}^{IJ}$ has a′ symmetry. It is important to note that this symmetry does not arise a priori from the calculation. $\boldsymbol{\tau}_x$, determined by a numerical procedure that does not enforce symmetry, is planar to an excellent approximation. However, since the electronic states are (nearly) degenerate, the symmetrical $\mathbf{g}^{IJ}$ and $\mathbf{h}^{IJ}$ in Figure 2 are mixed by the small deviation from planarity. The observed symmetry is restored by the following simple orthogonalization procedure.[105]

In general, $\mathbf{g}^{IJ}$ and $\mathbf{h}^{IJ}$ constructed from eqs 5a−c need not be orthogonal. This results from the degeneracy $E_I^{0,a}(\boldsymbol{\tau}_x) = E_J^{0,a}(\boldsymbol{\tau}_x)$ as a result of which the orthonormal eigenfunctions, $\mathbf{c}^I(\boldsymbol{\tau}_x)$ and $\mathbf{c}^J(\boldsymbol{\tau}_x)$, are determined only up to a rotation by an angle β. These "nascent" $\mathbf{g}^{IJ}$ and $\mathbf{h}^{IJ}$ may not reflect the point group symmetry at $\boldsymbol{\tau}_x$ and may not appear to be continuous along the seam. These limitations can be avoided by exploiting the very the flexibility that created the problem.[105] Rotating the $\mathbf{c}^I(\boldsymbol{\tau}_x)$ and $\mathbf{c}^J(\boldsymbol{\tau}_x)$ by angle β

$$\begin{pmatrix}\bar{\mathbf{c}}_I\\ \bar{\mathbf{c}}_J\end{pmatrix} = \begin{pmatrix}\cos\beta & -\sin\beta\\ \sin\beta & \cos\beta\end{pmatrix}\begin{pmatrix}\mathbf{c}_I\\ \mathbf{c}_J\end{pmatrix} = \mathbf{O}^{(2)}(\beta)\begin{bmatrix}\mathbf{c}_I\\ \mathbf{c}_J\end{bmatrix} \tag{6a}$$

transforms $\mathbf{g}^{IJ}$ and $\mathbf{h}^{IJ}$ to $\boldsymbol{\gamma}^{IJ}$ and $\boldsymbol{\eta}^{IJ}$ where

$$\boldsymbol{\gamma}^{IJ} = (\mathbf{g}^{IJ}\cos 2\beta + \mathbf{h}^{IJ}\sin 2\beta) \quad \text{and}$$
$$\boldsymbol{\eta}^{IJ} = (\mathbf{h}^{IJ}\cos 2\beta - \mathbf{g}^{IJ}\sin 2\beta) \tag{6b}$$

Then requiring that $\boldsymbol{\gamma}^{IJ}\cdot\boldsymbol{\eta}^{IJ} = 0$ gives for β

$$\tan 4\beta_0 = \frac{2[\mathbf{h}^{IJ}\cdot\mathbf{g}^{IJ}]}{[||\mathbf{h}^{IJ}||^2 - ||\mathbf{g}^{IJ}||^2]} \tag{6c}$$

Since $\tan(\alpha + m\pi) = \tan\alpha$ for $m = 0, \pm1, \pm2, \ldots$, and noting that 2β is required to evaluate $\boldsymbol{\gamma}^{IJ}$ and $\boldsymbol{\eta}^{IJ}$, the solutions of eq 6c, can be taken as $\beta = \beta_0 + m\,\pi/4$ for $m = \pm1, 2$. The $\mathbf{g}^{IJ}$ and $\mathbf{h}^{IJ}$ reported in Figures 2 and 4, were orthogonalized using eq 6c. The orthogonality constrained $\mathbf{g}^{IJ}$ and $\mathbf{h}^{IJ}$, which, as noted above, have the appropriate point group symmetry, greatly simplify the description of the seam of conical intersection.

Interestingly, from eq 6a $\mathbf{g}^{IJ}$ and $\mathbf{h}^{IJ}$ are interchanged via the transformation $\mathbf{O}^{(2)}(\pm\pi/4)$. This may seem counterintuitive since $\mathbf{g}^{IJ}$ is an energy difference gradient while $\mathbf{h}^{IJ}$ is a coupling term. In fact, this interchange is only possible at the conical intersection where it is simply a consequence of the degeneracy.

B. Noncrossing Rule. Conical intersections are not isolated points but are continuously connected, forming seams. The noncrossing rule, the classic 1929 theorem of Eugene P. Wigner and John von Neumann,[43] describes the dimensionality of the seam or, equivalently, the number of internal coordinates that must be simultaneously varied to locate a $\boldsymbol{\tau}_x$.

(i) Noncrossing Rule: A Dimensionality Theorem. According to the noncrossing rule *for a symmetric (hermitian) matrix, it is necessary to change two (three) parameters to achieve a pair*

TABLE 1: Noncrossing Rule[a]

$p_U(N)$	$d(N,m)$	$r_U(N,m)$	$p_H(N,m)$	$\Delta p_H(1,2)$
		H Hermitian		
N^2	$N-m+1$	m^2+N-m	N^2-m^2+1	3
		H Symmetric		
$\{N\}-N$	$N-m+1$	$\{m\}-m$	$\{N\}-\{m\}+1$	2

[a] $\{K\} = K(K+1)/2$, $\Delta p_H(m,n) = p_H(N,m) - p_H(N,n)$.

of degenerate eigenvalues. Interestingly, the validity of the noncrossing rule has been questioned on several occasions.[66,67,106] For this reason the simple yet elegant argument of Wigner and von Neumann is reproduced here on the basis of the translation of their work in ref 107.

In section II it was noted that the eigenvalues $E_I^{0,a}(\boldsymbol{\tau})$ of an hermitian matrix were not independent functions of $\boldsymbol{\tau}$. The essential idea in proof of Wigner and von Neumann is to use a representation for which the eigenvalues are in fact independent variables. Using this representation the number of independent parameters in **H** is determined, in the absence of any degeneracy, and with a single degeneracy. *The difference represents the number of parameters that may be changed to determine a degeneracy*.

The required representation is the "spectral representation" in which an N x N hermitian matrix is represented in terms of a unitary matrix $\mathbf{U}(\boldsymbol{\tau})$, $\mathbf{U}^\dagger\mathbf{U} = \mathbf{I}$, and a diagonal matrix **E** with diagonal elements $E_{PP} \equiv E_P$ by

$$H_{\alpha\beta}(\boldsymbol{\tau}) = \Sigma_{pq} U_{p\alpha}(\boldsymbol{\tau})^* E_p(\boldsymbol{\tau}) U_{p\beta}(\boldsymbol{\tau}) \tag{7}$$

The key point is that some **U** when used in eq 7 are redundant. To proceed, it is necessary to consider two cases, **H** is hermitian, complex-valued, with $H_{\alpha\beta}^* = H_{\beta\alpha}$, and **H** is symmetric, real-valued, with $H_{\alpha\beta} = H_{\beta\alpha}$. For the sake of brevity the results for **H** symmetric are placed in bold square brackets **[ ]**, immediately following the results for **H** hermitian.

When **H** is complex-valued **[**real-valued**]** **U** is unitary [orthogonal] and consists of $2N^2$ **[**N^2**]** real numbers, of which, since $\mathbf{U}^\dagger\mathbf{U} = \mathbf{I}$, N^2 **[**$N(N-1)/2$**]** are unique, that is **U** has N^2 [$N(N-1)/2$] independent parameters, $p_U(N) = N^2$ **[**$N(N-1)/2$**]**. See Table 1.

Since **U** appears quadratically in eq 7, not all **U** lead to distinct **H**. Consider, for the hermitian, and only the hermitian, case the nontrivial unitary matrix $\mathbf{U}^{(k)}$ given by

$$\mathbf{U}^{(k)}(\phi) = \begin{bmatrix} 1 & & & & & 0 \\ & 1 & & & & \\ & & e^{i\phi} & & & \\ & & & 1 & & \\ 0 & & & & & 1 \end{bmatrix} \tag{8a}$$

for, $k = 1, \ldots, N$. Inserting $\mathbf{U}^{(k)}$ into eq 7 leaves **H** unchanged. Thus, in the unitary [orthogonal] case for **E** nondegenerate or equivalently with an m-fold degeneracy for $m = 1$, there are N [0] redundant transformations, $r_U(N,m{=}1) = N$ **[0]**. See Table 1.

For *a single* m-fold degeneracy in **E**, with $m > 1$ the unitary [orthogonal] matrix with m^2 [$m(m-1)/2$] parameters

$$\mathbf{U}^{(j,k)} = \begin{bmatrix} 1 & & & & 0 \\ & 1 & & & \\ & & u_{11} & u_{12} & \\ & & u_{21} & u_{22} & \\ 0 & & & & 1 \end{bmatrix} \tag{8b}$$

leaves **H** unchanged since that portion of **E** is a constant times the $m \times m$ unit matrix. Thus, $r_U(N,m>1) = r_U(N-m,m{=}1) + m^2 = (N-m) + m^2$ **[**$m(m-1)/2$**]**. Finally, since here the unique elements of **E** are independent, **E** contains $d(N,m) = N - m + 1$ **[**$N - m + 1$**]** arbitrary parameters. Thus, the number of parameters in **H** of dimension N with a single *m-fold* degeneracy is $p_H(N,m) = p_U(N,m) + d(N,m) - r(N,m)$, which is given in Table 1. The number of free parameters in **H** at an intersection is, $\Delta p_H(1,2) = p_H(N,1) - p_H(N,2)$. See Table 1.

For the complex case $N = N$ and $m = 1$, $p_H(N,1) = N^2 + 1 - 1 = N^2$. This result could have been obtained more directly by noting that **H** has $2N(N-1)/2$ (off-diagonal real parameters) + N (diagonal real parameters) = N^2 (real parameters). For **H** real-valued $p_H(N,1) = N(N+1)/2 - 1 + 1 = N(N+1)/2$, again as expected. For $N = N$, and $m = m$ in the hermitian [symmetric] case $p_H(N,m) = N^2 - m^2 + 1$ **[**$N(N+1)/2 + 1 - m(m+1)/2$**]** parameters. Thus, one m-fold degeneracy renders $\Delta p_H(1,m) = m^2 - 1$ **[**$m(m+1)/2 - 1$**]** of the N^2 **[**$N(N-1)/2$**]** parameters arbitrary. The case $m = 2$ is of particular interest and yields 3 [2] as promised.

(ii) An Illustration: 2 × 2 Case. In the 2 × 2 case introduced in section II the degenerate hermitian [symmetric] matrix has $p_H(2,2) = 2^2 - 2^2 + 1 = 1$ [$3 - 3 + 1 = 1$] free parameter corresponding to the result

$$\mathbf{H} = \begin{bmatrix} E & 0 \\ 0 & E \end{bmatrix}$$

It is illuminating to consider this case in further detail. Noting that **E** can be written

$$\mathbf{E} = \begin{pmatrix} s & 0 \\ 0 & s \end{pmatrix} + \begin{pmatrix} -\epsilon & 0 \\ 0 & \epsilon \end{pmatrix} \tag{9a}$$

and restricting to the symmetric case where **U** is orthogonal from eq 7

$$\mathbf{H} = \begin{pmatrix} s & 0 \\ 0 & s \end{pmatrix} + \begin{pmatrix} \cos\phi & -\sin\phi \\ \sin\phi & \cos\phi \end{pmatrix} \begin{pmatrix} -\epsilon & 0 \\ 0 & \epsilon \end{pmatrix} \begin{pmatrix} \cos\phi & \sin\phi \\ -\sin\phi & \cos\phi \end{pmatrix} \tag{9b}$$

$$= \begin{pmatrix} s - \epsilon\cos 2\phi & -\epsilon\sin 2\phi \\ -\epsilon\sin 2\phi & s + \epsilon\cos 2\phi \end{pmatrix} \tag{9c}$$

Thus, as expected, **H** is defined by three parameters s, ϵ, and ϕ, and is degenerate provided $\epsilon = 0$, with $E = s$. Away from a degeneracy all three parameters are required to define **H**. However at the degeneracy, since $m = 2$, $r_U(2,2) = 2(2+1)/2 - 2 = 1$, one parameter of the orthogonal transformation, ϕ, becomes undefined, and $d(2,2) = 1$ (the choice of s). Further, when the seam is mapped out, since $p_H(2,2) = 1$, *one* parameter may be fixed (s) and, since $\Delta p_H(1,2) = 2$, *two* parameters (ϵ, ϕ) varied to achieve a degeneracy. Here, choice of parameters is not arbitrary, only s can be fixed and ϕ and ϵ must be varied. The search for degeneracies is not performed directly in the s, ϵ, and ϕ space but rather in the $\boldsymbol{\tau}$ space. This is permitted since $s = s(\boldsymbol{\tau})$, $\phi = \phi(\boldsymbol{\tau})$, and $\epsilon = \epsilon(\boldsymbol{\tau})$. However, in this case, a particular value of s cannot be specified; that is, s cannot be held fixed. If τ_k is the component of $\boldsymbol{\tau}$ to be held fixed the requirement $\partial s/\partial\tau_k \neq 0$ must hold.

(iii) Noncrossing Rule for Molecules with an Odd Number of Electrons. As pointed out in section IID for odd electron molecules in the absence of spatial symmetry, the seam of conical intersections has dimension $N^{int} - 5$ and has dimension $N^{C_s} - 3$ when C_s symmetry exists. It will prove illuminating below to point to the origin of the discrepancy with the results of the previous section. The key here is time reversal symmetry

as a consequence of which all eigenstates come in degenerate pairs. To accommodate this requirement, a basis in which the functions come in pairs, ψ_α and $T\psi_\alpha$, where T is the time reversal operator,[84] is used. A point of conical intersection is therefore a point of degeneracy 4. Naively applying the result of section IIIBii gives $4^2 - 1 = 15$, rather than the expected 5! The discrepancy arises from the fact that not all the matrix elements of **H** are independent, so that not all unitary transformations can be used to build **H**. In particular, using standard properties of the time reversal operator,[84] we find that

$$\langle\phi|\mathbf{H}\zeta\rangle = \langle T\phi|\mathbf{H}T\zeta\rangle^* \tag{10}$$

While the general case is not readily treated in this approach, the C_s result is straightforward. Rewrite eq 7 in block form

$$\mathbf{H} = \begin{pmatrix} \mathbf{U}^{II} & \mathbf{U}^{IT_I} \\ \mathbf{U}^{T_II} & \mathbf{U}^{T_IT_I} \end{pmatrix}^\dagger \begin{pmatrix} \epsilon & 0 \\ 0 & \epsilon \end{pmatrix} \begin{pmatrix} \mathbf{U}^{II} & \mathbf{U}^{IT_I} \\ \mathbf{U}^{T_II} & \mathbf{U}^{T_IT_I} \end{pmatrix} \tag{7'}$$

where $\boldsymbol{\epsilon}$ is a real-valued diagonal N x N matrix and, if $\langle\phi_i|\epsilon_j\rangle = U_{ij}^{II}$, then $\langle T\phi_i|T\epsilon_j\rangle = U_{ij}^{T_IT_I}$. When a plane of symmetry exists, all $(T\psi_\alpha,\psi_\beta)$ vanish by symmetry, giving $\mathbf{U}^{IT_I} = 0$ and $\mathbf{U}^{II*} = \mathbf{U}^{T_IT_I}$. Thus, **U** is determined by $\mathbf{U}^{II}$ so that the analysis of section IIIBii can be used and $\Delta p_H(1,2) = 3$. For a treatment of the no symmetry case see ref 108.

C. Algorithm for Locating Conical Intersections. The noncrossing rule describes the dimensionality of the intersection space and prescribes limits on how to search for a point of intersection. It does not, however, provide a means for locating points in that space. Several approaches for locating individual points of conical intersection currently exist.[68,109] Below is described the algorithm we have developed.

Assume $\boldsymbol{\tau}$ is near but not at $\boldsymbol{\tau}_x$, that is $\boldsymbol{\tau} + \delta\boldsymbol{\tau} = \boldsymbol{\tau}_x$. Expand $\mathbf{H}^{\mathrm{el},0}(\boldsymbol{\tau})$ in a Taylor series about $\boldsymbol{\tau}$:

$$\mathbf{H}^{\mathrm{el},0}(\boldsymbol{\tau} + \delta\boldsymbol{\tau}) \approx \mathbf{H}^{\mathrm{el},0}(\boldsymbol{\tau}) + \nabla_{\boldsymbol{\tau}}\mathbf{H}^{\mathrm{el},0}(\boldsymbol{\tau})\,\delta\boldsymbol{\tau} \tag{11a}$$

Taking matrix elements with $(\mathbf{c}^I(\boldsymbol{\tau}),\mathbf{c}^J(\boldsymbol{\tau}))$ gives the 2×2 matrix

$$\mathbf{H}^{\mathrm{el},0}(\boldsymbol{\tau} + \delta\boldsymbol{\tau}) = (E_{IJ}^{\mathrm{avg}}(\boldsymbol{\tau}) + \mathbf{s}^{IJ}(\boldsymbol{\tau})\cdot\delta\boldsymbol{\tau})\boldsymbol{I} + (\Delta\boldsymbol{E}_{IJ}(\boldsymbol{\tau}) + \mathbf{g}^{IJ}(\boldsymbol{\tau})\cdot\delta\boldsymbol{\tau})\boldsymbol{\sigma}_z + \mathbf{h}^{IJ}(\boldsymbol{\tau})\cdot\delta\boldsymbol{\tau}\boldsymbol{\sigma}_x \tag{11b}$$

where $\Delta E_{IJ} = E_I^{0,\mathrm{a}} - E_J^{0,\mathrm{a}}$ and **I** is a 2×2 unit matrix. $\mathbf{H}^{\mathrm{el},0}(\boldsymbol{\tau}_x)$ will have degenerate roots provided

$$H_{IJ}^{\mathrm{el},0}(\boldsymbol{\tau}+\delta\boldsymbol{\tau}) = 0 \qquad \text{and} \qquad H_{II}^{\mathrm{el},0}(\boldsymbol{\tau}+\delta\boldsymbol{\tau}) - H_{JJ}^{\mathrm{el},0}(\boldsymbol{\tau}+\delta\boldsymbol{\tau}) = 0 \tag{12}$$

which using eq 11 becomes

$$\mathbf{h}^{IJ}(\boldsymbol{\tau})\cdot\delta\boldsymbol{\tau} = 0 \qquad \text{and} \qquad \Delta\mathbf{E}_{IJ}(\boldsymbol{\tau}) = -\mathbf{g}^{IJ}(\boldsymbol{\tau})\cdot\delta\boldsymbol{\tau} \tag{13}$$

Equation 13 is the basis for an efficient algorithm for locating $\boldsymbol{\tau}_x$. However, these equations determine only two components of $\delta\boldsymbol{\tau}$, as required by the noncrossing rule. Thus, $\delta\boldsymbol{\tau}$ is underdetermined. The remaining $\delta\boldsymbol{\tau}$ can be determined using either or both (i) geometric constraints $C_I(\boldsymbol{\tau}) = 0$ and (ii) energy minimization. We implement these additional constraints using Lagrange multipliers. The functional

$$L^{IJ}(\boldsymbol{\tau},\boldsymbol{\xi},\boldsymbol{\lambda}) = E_I^{\mathrm{a}}(\boldsymbol{\tau}) + \xi_1\Delta E_{IJ}(\boldsymbol{\tau}) + \xi_2\mathbf{H}_{IJ}^{\mathrm{el},0}(\boldsymbol{\tau}) + \boldsymbol{\lambda}^\dagger\cdot\mathbf{C} \tag{14}$$

is expanded to second order and an extremum is sought with respect to $\boldsymbol{\tau}$ and the Lagrange multipliers $\boldsymbol{\xi}$ and $\boldsymbol{\lambda}$, giving

$$\begin{bmatrix} \mathbf{Q}^{IJ}(\boldsymbol{\tau},\boldsymbol{\xi},\boldsymbol{\lambda}) & \mathbf{g}^{IJ}(\boldsymbol{\tau}) & \mathbf{h}^{IJ}(\boldsymbol{\tau}) & \mathbf{k}(\boldsymbol{\tau}) \\ \mathbf{g}^{IJ}(\boldsymbol{\tau})^\dagger & 0 & 0 & \mathbf{0} \\ \mathbf{h}^{IJ}(\boldsymbol{\tau})^\dagger & 0 & 0 & \mathbf{0} \\ \mathbf{k}(\boldsymbol{\tau})^\dagger & \mathbf{0}^\dagger & \mathbf{0}^\dagger & \mathbf{0} \end{bmatrix} \begin{bmatrix} \delta\boldsymbol{\tau} \\ \delta\xi_1 \\ \delta\xi_2 \\ \delta\boldsymbol{\lambda} \end{bmatrix} = -\begin{bmatrix} \mathbf{g}^I(\boldsymbol{\tau}) + \xi_1\mathbf{g}^{IJ}(\boldsymbol{\tau}) + \xi_2\mathbf{h}^{IJ}(\boldsymbol{\tau}) + \boldsymbol{\lambda}^\dagger\mathbf{k}(\boldsymbol{\tau}) & \text{(15a)} \\ \Delta E_{IJ}(\boldsymbol{\tau}) & \text{(15b)} \\ 0 & \text{(15c)} \\ \mathbf{C}(\boldsymbol{\tau}) & \text{(15d)} \end{bmatrix}$$

where $\mathbf{Q}^{IJ}(\boldsymbol{\tau},\boldsymbol{\xi},\boldsymbol{\lambda}) = \nabla_{\boldsymbol{\tau}}\nabla_{\boldsymbol{\tau}}L^{IJ}$ and $\mathbf{k}(\boldsymbol{\tau}) = \nabla_{\boldsymbol{\tau}}\mathbf{C}(\boldsymbol{\tau})$. Note that eqs 15b and 15c are eq 13 and eq 15d imposes the constraints while the first equation minimizes the constrained energy. Table 2 illustrates the convergence properties of this algorithm for a $\boldsymbol{\tau}_x$ in HNCO. The adiabatic states are described using an expansion comprising $\sim 3.5 \times 10^6$ CSFs. The convergence is seen to be quite rapid.

TABLE 2: For HNCO, Convergence to $\boldsymbol{\tau}_x$ on Planar Trans Seam with $R(\mathrm{C-N}) = 2.65a_0$ from $\boldsymbol{\tau}_x$ with $R(\mathrm{C-N}) = 2.85a_0$

R(CN)	R(CO)	∠NCO	E_x (cm^{-1})	ΔE (cm^{-1})	norm[a]
2.8500	2.3321	103.00	5907.4		0.1102(1)
2.6573	2.3645	98.80	8222.9	151.91	0.4215(−2)
2.6501	2.3609	98.10	8833.9	5.9057	0.7595(−2)
2.6501	2.3568	98.20	8811.3	44.898	0.8324(−2)
2.6500	2.3594	98.20	8855.3	8.0157	0.5795(−2)
2.6500	2.3588	98.00	8835.6	1.9092	0.2435(−2)
2.6500	2.3579	98.20	8836.6	0.63871	0.8132(−3)

[a] Norm is norm of right-hand side of eq 15. Characteristic base 10 in parentheses.

D. Energies, Derivative Couplings, and Diabatic Bases. *(i) Energies and Derivative Couplings Using Intersection Adapted Coordinates.* In the adiabatic representation nonadiabatic transitions are driven by the derivative coupling,

$$f_\tau^{JI}(\boldsymbol{\tau}) = \left\langle \Psi_J^{0,\mathrm{a}}(\mathbf{r};\mathbf{R}) \middle| \frac{\partial}{\partial\tau} \Psi_I^{0,\mathrm{a}}(\mathbf{r};\mathbf{R}) \right\rangle_{\mathbf{r}} \tag{16a}$$

At a conical intersection the derivative coupling is singular. To quantify the propensity for a nonadiabatic transition, requires, at minimum, the singular component(s) of the derivative coupling and the energies. The importance of the parameters $\mathbf{s}^{IJ}$, $\mathbf{g}^{IJ}$, and $\mathbf{h}^{IJ}$ introduced previously is that they determine both the singular component of the derivative coupling and the linear or conical portion of the energy at $\boldsymbol{\tau}_x$. This can be shown using a degenerate perturbation theory originally used by Mead to describe X_3 systems.[38] In particular,[47] for $\boldsymbol{\tau}$ near a $\boldsymbol{\tau}_x$ and in the $g-h$ plane, $E_k^{0,\mathrm{a},(1)}(\boldsymbol{\tau})$, the linear part of the electronic energy, $E_K^{0,\mathrm{a}}(\boldsymbol{\tau})$, $K = I, J$, can be expressed in terms of g, h or d_{gh}, Δ_{gh} and $s_x = \mathbf{s}^{IJ}\cdot\mathbf{x}$, $s_y = \mathbf{s}^{IJ}\cdot\mathbf{y}$, by

$$\begin{pmatrix} E_I^{0,\mathrm{a},(1)} & 0 \\ 0 & E_J^{0,\mathrm{a},(1)} \end{pmatrix} = \rho(s_x\cos\phi + s_y\sin\phi)\mathbf{I} - \rho q_\Delta(\phi)\boldsymbol{\sigma}_z \tag{17a}$$

where

$$q(\phi)^2 = g^2\cos^2\phi + h^2\sin^2\phi = d_{gh}{}^2(1 + \Delta_{gh}\cos 2\phi)/2 = d_{gh}{}^2 q_\Delta(\phi)^2 \tag{17b}$$

Further, the singularity in the derivative coupling is restricted

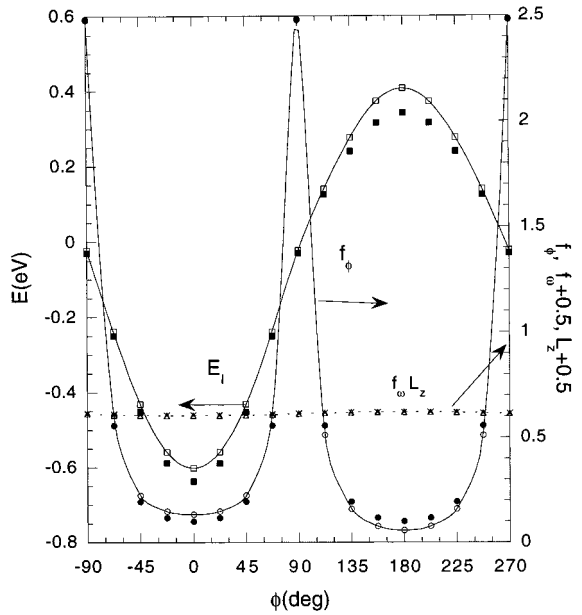

Figure 7. For HNCO: Electronic matrix elements along a circle centered at the conical intersection in Figure 2 with $\rho = 0.1a_0$. $E^{0,a}_{1^1A}$ and f_ϕ, the component of the derivative coupling that is singular at the conical intersection from ab initio wave functions (open symbols with lines) and perturbation theory (filled symbols). f_ω (open triangles with lines) derivative coupling with respect to a rotation about the *Z*-axis passing through the center of mass and the equivalent L_z (×'s).

to the ϕ component and is given by

$$(1/\rho)\, f^{JI}_{\phi} \approx (1/\rho)\, f^{JI,(1)}_{\phi} \equiv gh/(2\rho q(\phi)^2) = (g/h + h/g)q_\Delta(\phi)^2 = 1/(2\rho)\frac{\partial}{\partial\phi}\lambda(\phi) \quad (16b)$$

where

$$g\cos\phi = q(\phi)\cos\lambda(\phi) \qquad \text{and} \qquad h\sin\phi = q(\phi)\sin\lambda(\phi) \quad (16c)$$

Note that both the derivative coupling and the energy difference are expressed in terms of *g* and *h*. This reflects the fact that these quantities are not independent but are related to each other using, for example, perturbation theory. Figure 7 illustrates the use of eqs 17a and 16b reporting, for the conical intersection given in Figure 2, the $E^{0,a}_I$ and f^{IJ}_ϕ, obtained from the ab initio wave functions and compares them with the perturbative results $E^{0,a,(1)}_1$ and $f^{IJ,(1)}_\phi$. In this figure $\rho = 0.1a_0$ and $\phi = 0, ..., 2\pi$. The agreement between the ab initio quantities and their perturbative approximations, which require virtually no time to evaluate, is seen to be excellent. Thus, close to a conical intersection, the perturbative results can be used in lieu of costly ab initio calculations.

(ii) Confirming the Existence of a Conical Intersection. It is interesting to observe that the circulation, the line integral[92] around a closed loop, satisfies

$$\oint f^{IJ}_\phi(\phi)\, \mathrm{d}\phi \sim \pi \quad (18a)$$

This is to be expected since from eqs 16b and 16c as $\rho \to 0$

$$\oint f^{IJ}_\phi(\phi)\, \mathrm{d}\phi \xrightarrow{\rho\to 0} 1/2\int_0^{2\pi}\frac{\mathrm{d}\lambda(\phi)}{\mathrm{d}\phi}\,\mathrm{d}\phi = \pi \quad (18b)$$

Had the loop not contained a singularity (conical intersection) this circulation would have to approach zero as $\rho \to 0$. These observations are significant since conical intersections determined from numerical procedures are never exactly degenerate. The verification of eq 18b provides a computationally expedient method for proving the existence of a conical intersection.

There is one caveat, the quadrature in eq 18a is sensitive to the sign of f^{IJ}_ϕ when $|f^{IJ}_\phi|$ is small, in Figure 7 near $\phi = 0, \pi$. However, this sign can be determined, without determining a large number of points, using the fact that the derivative couplings with respect to noninternal coordinates are slowly varying near a conical intersection.[110] The evaluation of these derivative couplings, which also provides a stringent check of the algorithm for evaluating the $f^{IJ}_{\boldsymbol{\tau}}$, is briefly described below.

(iii) Derivative Couplings with Respect to Noninternal Coordinates. The f^{IJ}_κ are nonvanishing for $\kappa = \boldsymbol{\tau}$, an internal coordinate, as well as for $\kappa = O^{\mathrm{nuc}}$, an overall rotation or translation of the nuclei. However, unlike $f^{IJ}_{\boldsymbol{\tau}}$, $f^{IJ}_{O^{\mathrm{nuc}}}$ can be expressed as the matrix element of an electronic operator. This can be readily demonstrated as follows. Define $\mathbf{O}^k = \sum_{j=1}^{N^k}\mathbf{o}^k_j$ and $\mathbf{o}^k_j = r^k_j \mathrm{i}p^k_j$ or $\mathbf{o}^k_j = \mathrm{i}\mathbf{p}^k_j$, k = nuc, el. Then, since space is homogeneous, $[H^{\mathrm{el}}, O_\gamma] = 0$ where $\mathbf{O} = \mathbf{O}^{\mathrm{el}} + \mathbf{O}^{\mathrm{nuc}}$, and since $E^{0,a}_I$ depends only on $\boldsymbol{\tau}$

$$O_\gamma(H^{\mathrm{el},0} - E^{0,a}_I(\boldsymbol{\tau}))\Psi^{0,a}_I = (H^{\mathrm{el}} - E^{0,a}_I(\boldsymbol{\tau}))O_\gamma\Psi^{0,a}_I = 0 \quad (19a)$$

taking the matrix element with $\Psi^{0,a}_J$, $I \neq J$ gives

$$\langle\Psi^{0,a}_J|O_\gamma|\Psi^{0,a}_I\rangle(E^{0,a}_J - E^{0,a}_I) = 0 \quad (19b)$$

so that $\langle\Psi^{0,a}_J|O_\gamma|\Psi^{0,a}_I\rangle = 0$ and

$$O^{\mathrm{el}}_{\gamma,JI} = -\langle\Psi^{0,a}_J|O^{\mathrm{el}}_\gamma|\Psi^{0,a}_I\rangle = \langle\Psi^{0,a}_J|O^{\mathrm{nuc}}_\gamma|\Psi^{0,a}_I\rangle \equiv f^{JI}_{O^{\mathrm{nuc}}_\gamma} \quad (19c)$$

Thus, the derivative coupling with respect to an overall nuclear rotation (translation) is given by −i times the corresponding matrix element of the *electronic* angular (linear) momentum operator. This equivalence provides a stringent test of the algorithm used to evaluate $\mathbf{f}^{IJ}$. For $O^{\mathrm{nuc}}_\gamma = \omega$, a rotation about the *Z*-axis, O^{el} is L_z, the electronic orbital angular momentum about the *Z*-axis. Figure 7 compares f^{IJ}_ω and $L_{z,IJ}$.

In ref 110 it is shown that $L_{z,IJ}$ is slowly varying and nonnegligible near a conical intersection. Thus, its continuity can be used to enforce continuity on the remaining derivative coupling. This point is also illustrated in Figure 7.

(iv) Approximate Diabatic Bases near a Conical Intersection. The elimination of the singular part of the derivative coupling is an essential property of any diabatic basis. Indeed, recently a promising hybrid adiabatic/diabatic states approach to nonadiabatic dynamics has been suggested in which the *only* requirement on the diabatic states is that they eliminate the singularity in the derivative coupling.[75] A hybrid adiabatic/diabatic states approach can also be found in ref 111.

As the perturbation theory described above reproduces the derivative coupling, it can also be used to eliminate it. In particular, the transformation

$$\begin{pmatrix}\Psi^{0,a}_I\\ \Psi^{0,a}_J\end{pmatrix} = \begin{pmatrix}\cos\Theta & -\sin\Theta\\ \sin\Theta & \cos\Theta\end{pmatrix}\begin{pmatrix}\Psi^{0,d}_I\\ \Psi^{0,d}_J\end{pmatrix} \quad (20)$$

where $\Theta = \lambda(\phi)/2$, eliminates the $(1/\rho)$ contribution to the

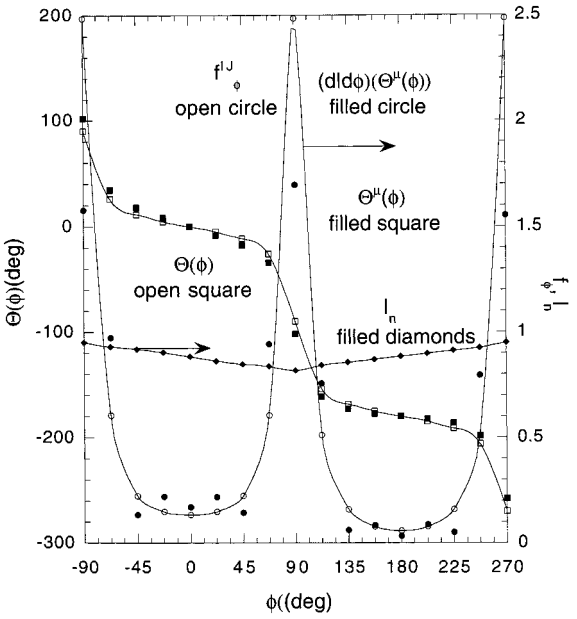

Figure 8. For HNCO: Analysis of dipole moment diabatization. Electronic matrix elements along a circle centered at the conical intersection in Figure 2. Reported are $\Theta^{\mu}(\phi)$, $\Theta(\phi) = (\pi - \alpha - \lambda(\phi))/2$), I_n (in eq 24c), the approximate derivative coupling $\partial/\partial\phi\ \Theta^{\mu} \equiv f_{\phi}^{\mu,IJ}$ and the derivative coupling computed from ab initio wave functions, f_{ϕ}^{IJ}.

derivative coupling and produces a diabatic Hamiltonian of the form

$$\mathbf{H}^{\mathrm{el,d}} = (s_x x + s_y y)\mathbf{I} - gx\boldsymbol{\sigma}_z + hy\boldsymbol{\sigma}_x \tag{21}$$

Extensions of this expression to higher powers in ρ have been reported.[105]

Approximate diabatic states can also be constructed by requiring smoothness of a molecular property. We have shown that the rotation angle $\Theta = \Theta^A$ in eq 23 below eliminates the singularity[110] in the derivative coupling. To see this, let $A^{\mathrm{el}}(\boldsymbol{r})$ be any hermitian (property) operator and define

$$A_{KL}(\boldsymbol{\tau}) = \langle \Psi_K^{0,\mathrm{a}}(\mathbf{r};\mathbf{R}) | A^{\mathrm{el}}(\mathbf{r}) \Psi_L^{0,\mathrm{a}}(\mathbf{r};\mathbf{R}) \rangle_{\mathbf{r}} \tag{22}$$

$$\tan 2\Theta^A(\boldsymbol{\tau}) = \frac{2A_{IJ}(\boldsymbol{\tau})}{A_{JJ}(\boldsymbol{\tau}) - A_{II}(\boldsymbol{\tau})} \tag{23}$$

Then provided the numerator and denominator do not vanish simultaneously as $\boldsymbol{\tau} \rightarrow \boldsymbol{\tau}_x$

$$2\Theta^A(\phi) = n\pi - \alpha - \lambda(\phi), \qquad n = 0, \pm 1, \ldots \tag{24a}$$

where the constant offset, α, is given by

$$\tan \alpha = 2A_{IJ}(\boldsymbol{\tau}_x)/(A_{II}(\boldsymbol{\tau}_x) - A_{JJ}(\boldsymbol{\tau}_x)) \tag{24b}$$

Thus, $-\Theta^A$ differs by a constant from $\lambda(\phi)/2$, the perturbation theory result. These results are illustrated in Figure 8. which reports $-\Theta^A$ and $\lambda(\phi)/2$, and the "invariant",

$$I_n \equiv (2\Theta^A(\phi) + \alpha + \lambda(\phi))/\pi = n \tag{24c}$$

Note the good agreement between $\Theta^{\mu}(\phi)$ and $\Theta(\phi) = (\pi - \alpha - \lambda(\phi))/2$, and between the approximate derivative coupling $(\partial/\partial\phi)\Theta^{\mu}(\phi) \equiv f_{\phi}^{\mu,IJ}$ and the computed derivative coupling f_{ϕ}^{IJ}.

TABLE 3: C_s Double Group

	E	$R = \sigma^2$	σ	$R\sigma$
a′	1	1	1	1
a″	1	1	−1	−1
e′	1	−1	i	−i
e″	1	−1	−i	i

These observations reflect eq 24a, which shows that the transformation to diabatic states generated by eqs 22 and 23 rigorously removes the singularity in the derivative coupling at the conical intersection.

E. Spin−Orbit Effect and the Noncrossing Rule. When the spin−orbit interaction is included, the electronic Hamiltonian may become complex-valued. When this occurs, both the dimensionality of the seam of conical intersection[43] and the geometric phase effect[39] are altered. This does *not* occur for molecules with an even number of electrons. For even electron molecules Wigner observed that the matrix elements of $\mathbf{H}^{\mathrm{el}} = \mathbf{H}^{\mathrm{el},0} + \mathbf{H}^{\mathrm{so}}$ can be chosen real,[112] so that conical intersections for $\mathbf{H}^{\mathrm{el}}$ obey the same equations as those for $\mathbf{H}^{\mathrm{el},0}$. However, for molecules with an odd number of electrons, the focus here, $\mathbf{H}^{\mathrm{el}}$ cannot in general be chosen real-valued. Here we illustrate the changes in the seam of conical intersection and the geometric phase that arise when the spin−orbit interaction is included the nonrelativistic Hamiltonian. The spin−orbit interaction is incorporated in a perturbative manner.[113] This analysis will be relevant to the formation of the van der Waals complex[114,115] $\mathrm{Al}(^2\mathrm{P}) + \mathrm{H}_2 \rightarrow \mathrm{Al{-}H}_2$ and the quenching reaction[116,117] $\mathrm{OH}(^2\Sigma^+) + \mathrm{H}_2 \rightarrow \mathrm{OH}(^2\Pi) + \mathrm{H}_2$, problems of considerable current interest.

We begin by reviewing the electronic structure description of these states in the presence of the spin−orbit interaction. In C_s symmetry a ^{2}P state or the pair of states ($^2\Sigma^+$, $^2\Pi$) reduces to two ^{2}A′ and one ^{2}A″ states. The six states can be transformed to a time reversal adapted basis $\Psi_{ne'}^{\mathrm{e},0} = T\Psi_{ne''}^{\mathrm{e},0}$ as shown in

$$\Psi$$

$$1^2\mathrm{A}' \qquad \sqrt{2}\Psi_{1\mathrm{e}'}^{\mathrm{e},0} = \Psi_{1^2\mathrm{A}'(1/2)}^{0,\mathrm{a}} + \mathrm{i}\Psi_{1^2\mathrm{A}'(-1/2)}^{0,\mathrm{a}} \tag{25a′}$$

$$2^2\mathrm{A}' \qquad \sqrt{2}\Psi_{2\mathrm{e}'}^{\mathrm{e},0} = \Psi_{2^2\mathrm{A}'(1/2)}^{0,\mathrm{a}} + \mathrm{i}\Psi_{2^2\mathrm{A}'(-1/2)}^{0,\mathrm{a}} \tag{25b′}$$

$$1^2\mathrm{A}'' \qquad \sqrt{2}\Psi_{3\mathrm{e}'}^{\mathrm{e}} = \Psi_{1^2\mathrm{A}''(1/2)}^{0,\mathrm{a}} - \mathrm{i}\Psi_{1^2\mathrm{A}''(-1/2)}^{0,\mathrm{a}} \tag{25c′}$$

$$T\Psi$$

$$1^2\mathrm{A}' \qquad -\mathrm{i}\sqrt{2}\Psi_{1\mathrm{e}''}^{\mathrm{e},0} = \Psi_{1^2\mathrm{A}'(1/2)}^{0,\mathrm{a}} - \mathrm{i}\Psi_{1^2\mathrm{A}'(-1/2)}^{0,\mathrm{a}} \tag{25a″}$$

$$2^2\mathrm{A}' \qquad -\mathrm{i}\sqrt{2}\Psi_{2\mathrm{e}'}^{\mathrm{e},0} = \Psi_{2^2\mathrm{A}'(1/2)}^{0,\mathrm{a}} - \mathrm{i}\Psi_{2^2\mathrm{A}'(-1/2)}^{0,\mathrm{a}} \tag{25b″}$$

$$1^2\mathrm{A}'' \qquad -\mathrm{i}\sqrt{2}\Psi_{3\mathrm{e}''}^{\mathrm{e}} = \Psi_{1^2\mathrm{A}''(1/2)}^{0,\mathrm{a}} + \mathrm{i}\Psi_{1^2\mathrm{A}''(-1/2)}^{0,\mathrm{a}} \tag{25c″}$$

Here $\Psi_{I^2\mathrm{A}(M_s)}^{0,\mathrm{a}}$ is the I^2A adiabatic eigenstate of the nonrelativistic (Coulomb) Hamiltonian with M_s given parenthetically. The $\Psi_{\mathrm{Ib}}^{\mathrm{e}}$ carry the b = e′ or e″ representations, the distinct double-valued irreducible representations of the C_s double group related by complex conjugation. See Table 3.

$\mathbf{H}^{\mathrm{el}}(\mathrm{e}')$ and $\mathbf{H}^{\mathrm{el}}(\mathrm{e}'')$, the Hamiltonian matrices corresponding to the Ψ and $T\Psi$ sets of eq 25, respectively, are therefore degenerate and uncoupled and $\mathbf{H}^{\mathrm{el}}(\mathrm{e}'') = \mathbf{H}^{\mathrm{el}}(\mathrm{e}')^*$. See discussion following eq 7′. A general discussion of the locus of conical intersections for this Hamiltonian will be reported as part of a manuscript describing an analytic gradient driven algorithm for locating conical intersections in $\mathbf{H}^{\mathrm{el}}$.[100] Here, for simplicity, we restrict to the 1^2A′, 2^2A′ space, which can also have a conical intersection in the absence of spin−orbit coupling. For this

situation, which is encountered for C_{2v} symmetry in $Al-H_2$ and $OH-H_2$, $\mathbf{H}^{el}(e')$ is

$$\mathbf{H}^{el}(e') - \begin{pmatrix} E^{0,a}_{1^2A'} & -i\gamma \\ +i\gamma & E^{0,a}_{2^2A'} \end{pmatrix} \equiv s\mathbf{I} - \epsilon\boldsymbol{\sigma}_z + \gamma\boldsymbol{\sigma}_y \qquad (26)$$

where $i\gamma = \langle\Psi^{e,0}_{1e'}|\mathbf{H}^{so}|\Psi^{e,0}_{2e'}\rangle$, $\epsilon = (E^{0,a}_{2^2A'} - E^{0,a}_{1^2A'})/2$, $s = (E^{0,a}_{2^2A'} + E^{0,a}_{1^2A'})/2$, and γ is real-valued. $\mathbf{H}^{el}(e')$ can only have a degeneracy on s^0, the seam for $\mathbf{H}^{el,0}$, where ϵ is zero. This can be seen formally by observing that $\mathbf{H}^{el}(e')$ can be brought into diagonal form by the transformation

$$\mathbf{U} = \cos\theta\mathbf{I} + \sin\theta\boldsymbol{\omega} \qquad \text{where} \qquad \boldsymbol{\omega} = \begin{pmatrix} 0 & i \\ i & 0 \end{pmatrix} \qquad (27)$$

Noting that $\boldsymbol{\sigma}_z\boldsymbol{\omega} = -\boldsymbol{\sigma}_y$; $\boldsymbol{\omega}\boldsymbol{\sigma}_z = \boldsymbol{\sigma}_y$; $\boldsymbol{\sigma}_y\boldsymbol{\omega} = \boldsymbol{\sigma}_z$; $\boldsymbol{\omega}\boldsymbol{\sigma}_z = -\boldsymbol{\sigma}_y$; and $\boldsymbol{\omega}\boldsymbol{\omega}^* = \boldsymbol{\omega}\boldsymbol{\omega}^\dagger = \boldsymbol{I}$,

$$\mathbf{U}^\dagger\mathbf{H}^{el}\mathbf{U} = s\mathbf{I} + (-\epsilon\cos 2\theta + \gamma\sin 2\theta)\boldsymbol{\sigma}_z + (\epsilon\sin 2\theta + \gamma\cos 2\theta)\boldsymbol{\sigma}_x \qquad (28)$$

which is diagonal with eigenvalues

$$E_\pm = s \pm (\epsilon^2 + \gamma^2)^{1/2} \qquad (29)$$

provided the coefficient of $\boldsymbol{\sigma}_x$ vanishes, that is

$$\tan 2\theta = -\gamma/\epsilon \qquad (30)$$

From eq 29 a conical intersection exists at $\epsilon = \gamma = 0$. Since $\epsilon = 0$ this seam is a subset of s^0, and in the case of a triatomic, the seam is a single point. This is consistent with the noncrossing rule according to which the inclusion of the spin−orbit interaction reduces the seam of conical intersection from a line, $N^{int} - 2 = 1$ to a point $N^{int} - 3 = 0$.

F. Geometric Phase. The geometric phase effect was first observed for a symmetric Hamiltonian, by Longuet-Higgins,[37,118] as part of his studies of the Jahn−Teller effect. Let L be a closed loop beginning at $\mathbf{R}^0$, terminating at $\mathbf{R}^N = \mathbf{R}^0$ and containing a conical intersection. He observed that when an adiabatic wave function $\Psi^{0,a}_K(\mathbf{r};\mathbf{R})$, locally continuous in $\mathbf{R}$, is transported around such a loop, it changes sign; that is, it acquires a phase $\exp[-i\Omega_{KK}(L)]$, where $\Omega_{KK}(L) = \pi$

$$\Psi^{0,a}_I(\mathbf{r};\mathbf{R}^0) \xrightarrow{L} \exp(-i\Omega_{II}(L))\Psi^{0,a}_I(\mathbf{r};\mathbf{R}^N) \qquad (31)$$

The generalization to complex wave functions required to take account of the spin−orbit interaction was discussed by Stone.[97] Subsequently, Berry, provided a result in closed form for general nonadiabatic processes.[39] Berry concluded that

$$\Omega_{II}(L) = \oint_L d\boldsymbol{\tau}\,\langle\Psi^{e,a}_I|\nabla_{\boldsymbol{\tau}}\Psi^{e,a}_I\rangle_{\mathbf{r}} = \Omega/2 \qquad (32)$$

where Ω is the solid angle subtended by L at $\boldsymbol{\tau}_x$. See Figure 3.

Below the geometric phase is reviewed. Again, it is necessary to distinguish between the results for $\mathbf{H}^{el}$ symmetric, that is, real-valued and $\mathbf{H}^{el}$ hermitian, that is complex-valued. We begin with the case that $\mathbf{H}^{el}$ is symmetric and for simplicity use as adiabatic states the nonrelativistic eigenstates, $\Psi^{0,a}_K(\mathbf{r};\mathbf{R})$, the solutions to eq 3.

(i) $\boldsymbol{H^{el}}$ Symmetric. Near $\boldsymbol{\tau}_x$ a point of conical intersection $\mathbf{H}^{el,0}$ is given, without loss of generality, by

$$\mathbf{H}^{el,0}(x,y) = (s_x x + s_y y)I + gx\sigma_z + hy\sigma_x \qquad (33)$$

Using (ρ, ϕ), where $x = \rho\cos\phi$ and $y = \rho\sin\phi$, a circular loop L of radius ρ surrounding $\boldsymbol{\tau}_x$ has initial and final points, $\mathbf{R}^0 = (\rho, \phi)$ and $\mathbf{R}^N = (\rho, \phi + 2\pi)$ with ρ fixed. To see what happens to the eigenfunctions along this path, note the following: (i) that $\mathbf{H}^{el,0}$ in eq 33 can be brought into diagonal from by the transformation $\mathbf{O}^{(2)}(\lambda(\phi)/2)$ (see eq 6a), where $\lambda(\phi)$ is defined in eq 16c; (ii) that from eq 16c it can be shown that $\lambda(\phi + 2\pi)/2 = (\lambda(\phi) + 2\pi)/2 = \lambda(\phi)/2 + \pi$; and (iii) that $\mathbf{O}^{(2)}(\pi) = -\boldsymbol{I}$. Then the eigenfunction with lower energy satisfies

$$\Psi^{0,a}_I(\mathbf{r};\mathbf{R}^0) \equiv \cos(\lambda(\phi)/2)\Psi^{0,a}_I(\mathbf{r};\mathbf{R}_x) - \sin(\lambda(\phi)/2)\Psi^{0,a}_J(\mathbf{r};\mathbf{R}_x) \qquad (34a)$$

$$\begin{aligned}\Psi^{0,a}_I(\mathbf{r};\mathbf{R}^N) &\equiv \cos(\lambda(\phi)/2 + \pi)\Psi^{0,a}_I(\mathbf{r};\mathbf{R}_x) - \sin(\lambda(\phi)/2 + \pi)\Psi^{0,a}_J(\mathbf{r};\mathbf{R}_x) \\ &= \cos(\lambda(\phi)/2 + \pi)\Psi^{0,a}_I(\mathbf{r};\mathbf{R}_x) - \sin(\lambda(\phi)/2 + \pi)\Psi^{0,a}_J(\mathbf{r};\mathbf{R}_x) \\ &= -\Psi^{0,a}_I(\mathbf{r};\mathbf{R}^0) \qquad (34b)\end{aligned}$$

that is $\Psi^a_I(\mathbf{r};\mathbf{R}^0) \xrightarrow[L]{} -\Psi^a_I(\mathbf{r};\mathbf{R}^0)$ so that $\Omega_{II}(L) = \pi$. This is the geometric phase effect. In this case $\Psi^a_I(\mathbf{r};\mathbf{R})$ is *double-valued* as a function of $\mathbf{R}$; that is, for any $\mathbf{R}$ the sign of Ψ^a_I is indeterminant since it depends on the path to that point!

(ii) $\boldsymbol{H^{el}}$ Hermitian. Here we consider $\mathbf{H}^{el}(e')$ in eq 26, extending an analysis due to Stone;[97] see also ref 119. The basis functions for $\mathbf{H}^{el}(e')$ are the nonrelativistic adiabatic states and exhibit a geometric phase effect with respect to s^0. See Figure 3. By using eq 27, the adiabatic wave functions including the spin−orbit effect are given by

$$\begin{pmatrix} \Psi^{e,a}_I \\ \Psi^{e,a}_J \end{pmatrix} = \begin{pmatrix} \cos\theta\tilde{\Psi}^{e,0}_{1e'} + i\sin\theta\tilde{\Psi}^{e,0}_{2e'} \\ i\sin\theta\tilde{\Psi}^{e,0}_{1e'} + \cos\theta\tilde{\Psi}^{e,0}_{2e'} \end{pmatrix} \qquad (35)$$

where $\tilde{\Psi}^{e,0}_{je'} = e^{i\Omega(\boldsymbol{\tau})}\tilde{\Psi}^{e,0}_{je'}$ and θ satisfies eq 30. Equation 35 will be used to determine $\Omega_{II}(L)$ and the derivative coupling.

As noted above, the geometric phase effect is intrinsically more complicated in the hermitian case. To evaluate $\Omega_{II}(L)$, $\Psi^{e,a}_I(\mathbf{r};\mathbf{R})$ must be chosen continuous. Here we require that $\langle\Psi^{e,a}_I(\mathbf{r};\mathbf{R}+\delta\mathbf{R})|\Psi^{e,a}_I(\mathbf{r};\mathbf{R})\rangle$ be real though first order, that is. $\mathrm{Im}\langle\delta\Psi^{e,a}_I(\mathbf{r};\mathbf{R})|\Psi^{e,a}_I(\mathbf{r};\mathbf{R})\rangle = 0$. Consider a loop around the z-axis pictured in Figure 3, sufficiently small that the $\Psi^{e,0}_{ie}$ are eigenfunctions of $\mathbf{H}^{el,0}$ in eq 33, Using eq 35 we find

$$\langle\Psi^{e,a}_I|\nabla\Psi^{e,a}_I\rangle_{\mathbf{r}} = i(1 - \sin 2\theta)\nabla(\lambda/2) \qquad (36a)$$

$$\langle\Psi^{e,a}_I|\nabla\Psi^{e,a}_J\rangle_{\mathbf{r}} = -\cos 2\theta(\nabla\lambda/2) - i\nabla\theta \qquad (36b)$$

Assume that $\gamma = \gamma(z)$ and that the distances have been scaled such that $\gamma = z$ and $\epsilon = \rho$. From the definition of the subtended angle

$$\begin{aligned}\Omega &= -\oint dS\,\mathbf{n}\cdot\mathbf{r}/r^3 = \oint dS\cos(\pi/2 - 2\theta)/r^2 \\ &= -\int\int d\phi\,\rho\,d\rho\,\frac{z}{(z^2+\rho^2)^{1/2}}\frac{1}{(z^2+\rho^2)} = \\ &\qquad -2[\pi(z/(z^2+\rho^2)^{1/2} - z/(z^2+0)^{1/2})] \\ &= 2\pi(1 - \sin 2\theta) \qquad (37)\end{aligned}$$

whereas using eq 36a the integrated phase is

$$\Omega_{II} = \oint \nabla(\lambda(\phi)/2)(1 - \sin 2\theta)\, \mathrm{d}\boldsymbol{\tau} = \int_0^{2\pi}(1 - \sin 2\theta)\, \mathrm{d}\phi\, \frac{\mathrm{d}}{\mathrm{d}\phi}(\lambda(\phi)/2) = \pi(1 - \sin 2\theta) \quad (38)$$

so that $\Omega_{II} = \Omega/2$, which is an example of Berry's geometric phase theorem. On the other hand, the circulation of the derivative coupling is, using eq 36b and noting that θ is constant along the loop

$$\oint(\cos 2\theta(\nabla\lambda/2) - \mathrm{i}\nabla\theta)\, \mathrm{d}\boldsymbol{\tau} = \int_0^{2\pi}\cos 2\theta\, \mathrm{d}\phi\frac{\mathrm{d}}{\mathrm{d}\phi}(\lambda(\phi)/2) = \pi \cos 2\theta \quad (39)$$

Thus, for the hermitian case the circulation of the derivative couplings does not equal the accumulated phase unless $2\theta = n\pi$; that is, the loop in Figure 3 must contain the point of conical intersection, in which case $\gamma(z)$ vanishes.

IV. Nuclear Dynamics Near Conical Intersections

As noted in the Introduction conical intersections can affect nuclear motion in diverse and novel ways. Below we consider two aspects of nonadiabatic transitions induced by conical intersections, the efficiency of UtL transitions for a vertical symmetric (Jahn−Teller) cone and the propensity for channeling of a wave packet following a LtU transition on a symmetric tilted cone. In the course of these discussions the question of the differences between same-symmetry conical intersections and the more standard, but comparatively rare symmetry-required (Jahn−Teller) intersections will be addressed. In order to isolate the effects of the conical intersection from those attributable to other regions of nuclear coordinate space, we consider the dynamics of wave packets originating in the vicinity of the conical intersection, with nuclear dynamics restricted to the $g-h$ plane.

A. Adiabatic State Formulation. Nuclear dynamics near conical intersections are determined from the solution of the time dependent Schrödinger equation

$$\left(\mathrm{i}\hbar\frac{\partial}{\partial t} - \mathbf{H}^{\mathrm{T}}\right)\Psi^{\mathrm{T,a}}(\mathbf{r};\rho,\phi,t) = 0 \quad (40)$$

using the Born−Huang approach for which

$$\Psi^{\mathrm{T,a}}(\mathbf{r},\rho,\phi,t) = \sum_{\alpha,K}\tilde{\Psi}^{\mathrm{a}}_K(\mathbf{r};\rho,\phi)\, \chi^{\mathrm{a},K}_\alpha(\rho,\phi)\, w^{\mathrm{a},K}_\alpha(t) \quad (41)$$

(ρ, ϕ) denote the nuclear coordinates in the $g-h$ plane introduced in section IIIA

$$\tilde{\Psi}^{\mathrm{a}}_K(\mathbf{r};\rho,\phi) = \mathrm{e}^{\mathrm{i}A(\phi)}\Psi^{0,\mathrm{a}}_K(\mathbf{r};\rho,\phi) \quad (42a)$$

and

$$\chi^{\mathrm{a},K}_\alpha(\rho,\phi) \rightarrow \tilde{\xi}^K_{m\nu}(\rho,\phi) = \rho^{1/2}\xi^K_{m\nu}(\rho)1/\sqrt{(2\pi)}\mathrm{e}^{\mathrm{i}m\phi} \quad (42b)$$

The form of the individual terms is key here. Since the origin is a point of conical intersection, $\Psi^{0,\mathrm{a}}_K(\mathbf{r};\rho,\phi)$ changes sign when $\phi \rightarrow \phi + 2\pi$. Therefore the geometric phase factor $\exp[\mathrm{i}A(\phi)]$ is included in eq 42a to make the *adiabatic* electronic wave function single-valued as a function of nuclear coordinates. This results in modifications to the coupled state nuclear Schrödinger equation. See eq A3 in the Appendix. Having made the electronic wave function single-valued, the nuclear wave functions can be constructed in a single-valued basis. Thus, in eq 42b m is an integer.

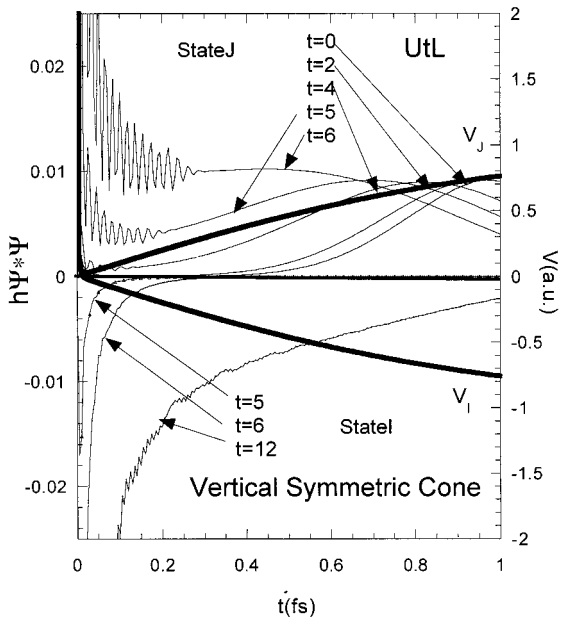

Figure 9. For the UtL transition, $h\Psi^*\Psi(L,\rho,\phi,t)$, where h is the grid spacing (independent of ϕ) superimposed on the potential $V^{\mathrm{sr},m}_{\pm} = \pm\rho + (m + {}^1/_2)^2/(2M\rho^2)$, with $V_I = V^{\mathrm{sr},0}_-$ and $V_J = V^{\mathrm{sr},0}_+$. For economy of presentation $-h\Psi^*\Psi(I,\rho,\phi,t)$ is reported, so that the state I (J) density appears on lower (upper) half.

B. Partitioning of $\mathbf{H}^{\mathrm{T}}$. The principal differences between a symmetry-required and a same-symmetry conical intersection are (i) in the later case Δ_{gh}, s_x, and s_y can be nonnzero and (ii) the phase angle $A(\boldsymbol{\tau})$ is more difficult to construct owing to the absence of symmetry. Both these problems can be addressed by rewriting the total Hamiltonian for a general conical potential so that it looks like the Hamiltonian for a symmetry-required conical intersection plus, a potential term depending on $S(x,y)$ and a kinetic term depending on Δ_{gh}, that is

$$\mathbf{H}^{\mathrm{T}} = \mathbf{H}^{\mathrm{sr}} + K^{\Delta} + V^{S} \quad (43)$$

where $\mathbf{H}^{\mathrm{sr}}$ is the Hamiltonian for a symmetry restricted (here the linear Jahn−Teller problem), K^{Δ} (V^S) is the part of the nuclear kinetic energy (potential energy) not included in $\mathbf{H}^{\mathrm{sr}}$. In eq 43 the superscript Δ (S) indicate that the term is nonvanishing only when Δ (S), is nonzero. The detailed description of the Hamiltonian is given the Appendix. There it is seen that $\mathbf{H}^{\mathrm{T}}$ depends on the quantity $(m + l + {}^1/_2)$, where l is an arbitrary integer and constitutes a gauge transformation, $\Psi^{\mathrm{T}}(\mathbf{r},\rho,\phi) \rightarrow \exp(\mathrm{i}l\phi)\Psi^{\mathrm{T}}(\mathbf{r},\rho,\phi)$. From the results of the Appendix we conclude that Ψ^{T} will be independent of this gauge transformation (provided the expansion in m is not truncated).

In the two examples that follow, the initial wave packet is taken as a symmetric Gaussian ring located on surface I (J) for a LtU (UtL) transition, with mass (M) 10 amu and exponential $-{}^1/_2\alpha(\rho - \rho_0)^2$, where $\alpha = 10.9$ and $\rho_0 = 1.0$. Further details can be found in ref 33. For the vertical symmetric cone $d_{gh} = 1$, while for the tilted cone $d_{gh} = 1$, and $s_x = 0.9$.

C. Downward Transitions through a Vertical Symmetric Cone. Valuable insights into near conical intersection dynamics are obtained from the vertical symmetric cone, which serves as the reference for other conical topographies. For a vertical symmetric conical intersection, since both the initial conditions and potential are independent of ϕ, $\Psi^*(K,\rho,\phi,t)\ \Psi(K,\rho,\phi,t) \equiv \Psi^*\Psi(K,\rho,\phi,t)$ is also. Figure 9 reports $\Psi^*\Psi$ superimposed on

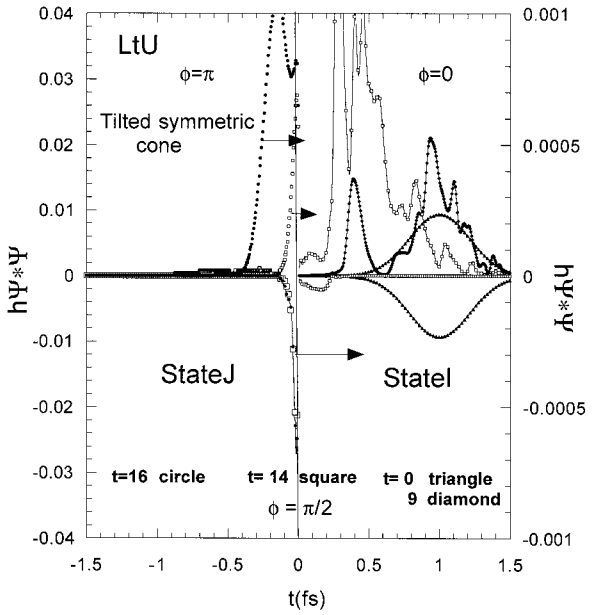

Figure 10. $h\Psi^*\Psi(L,\rho,\phi,t)$ LtU transition. $g = h = 1/\sqrt{2}s_x = 0.9$, $s_y = 0$. For economy of presentation, $\phi = 0$ is reported in the upper right quadrant, $\phi = \pi/2$ (lower half of figure) $-h\Psi^*\Psi(I,\rho,\phi,t)$ is reported; and for $\phi = \pi$ (upper left quadrant) $-\rho$ is used on the abscissa.

the adiabatic potential for a wave packet originating on surface *J*, the upper surface.

For $t \leq 2$ the packet maintains its shape, in the radial direction. This limited change in the wave packet's shape reflects the absence of a reflected wave. By $t = 4$ fs a scattered wave (from the inner wall) exists on surface *J* and (coherent) oscillations are observed on that potential energy surface. As time progresses, the portion of the wave packet on potential energy surface *J* becomes concentrated near the conical intersection. Significantly, no oscillations are observed on surface *I* (for $t < 12$ fs). This reflects the absence of a reflected wave. In other words, the portion of the wave packet in state *I* escapes directly from that region. The minor oscillations for $t = 12$ fs are most likely the result of small reflection effects, produced here by the hard wall at the right-hand boundary.

Thus, the lower cone is fully efficient in propagating the wave packet away from the conical intersection. It might be thought that the singularity in the derivative coupling at the conical intersection would lead to a fully efficient transfer of the wave packet from surface *J* to surface *I*. The existence of a reflected wave on surface *J* shows that this is not the case.

Recently, there has been considerable interest in the effect of not including the geometric phase in $\mathbf{H}^{T}$.[9,16,120,121] The present results offer some interesting insights in this regard. Omission of the geometric phase amounts to taking $l = {}^1/_2 + l'$ while *m* remains an integer. This is not a gauge transformation, and identical results cannot be expected. However, differences evident in practical examples maybe small. This need not be the case. From eq A7b it is seen that if the geometric phase had been omitted as described above and the gauge $l = -1$ were used, this wave packet would not decay at all!

D. Upward Transitions: The Importance of Tilt. By symmetry $\Psi^*\Psi(K,\rho,\pi/2,t) = \Psi^*\Psi(K,\rho,3\pi/2,t)$. Figure 10 reports $\Psi^*\Psi(K,\rho,\phi,t)$ for the LtU transition through the tilted symmetric cone defined above. Only $\phi = 0$, $\pi/2$ ($\pi/2,\pi$) are reported for state *I* (*J*), reflecting wave packet propagation to larger ρ for $\phi = \pi$ on surface *I* and the negligible contributions for $\phi = 0$ on surface *J*.

From Figure 10 a clear preference for $\phi = \pi$ is evident for the wave packet emerging in state *J*. Note that as the wave packet approaches the conical intersection on surface *I*, reflected wave induced oscillations are evident. Such oscillations occur to a much smaller extent on surface *J*, indicating largely unfettered escape, for $\phi = \pi$.

There are several factors that can affect the behavior of the wave packet near a conical intersection for tilted symmetric type double cones. Since *m* is no longer a good quantum number, the wave packet swirls down the upper cone and also swirls as its exits on the lower cone. For the tilted cone the preferred orientations are the same in the upper and lower cones, whereas for an asymmetric vertical cone they are complementary; that is, minima on the upper cone are the maxima on the lower cone. Compare Figure 5b,c.

The origin of the LtU transition for the tilted symmetric cone is seen from Figure 5c to be the favorable energetics along $\phi = 0$ on $E_I^{0,a}$. See solid arrow in Figure 5c. For this direction of approach, the wave packet emerges on the upper surface near $\phi = \pi$, which is the preferred direction for egress on the upper surface. Consistent with this observation $\Psi^*\Psi(J,\rho,\phi,t)$ finds its primary support for ϕ near π. Swirling on the lower surface from $\phi = 0$ toward $\phi = \pi/2$, $3\pi/2$ (Figure 10, $t = 9$ fs) leads to transitions onto the upper surface that continue to swirl toward $\phi = \pi$. Compare the $t = 14$ and 16 fs results in state *I* for $\phi = \pi/2$, π.

V. Unanswered Questions

A. Intersecting Seams. Conical intersections are intersections of potential energy surfaces. It had been shown that in some triatomic molecules,[122−125] all of which had C_{2v} or higher symmetry, an intersection or confluence of a symmetry-allowed seam of conical intersection and a seam of conical intersection of two states of the same-symmetry (a same-symmetry seam) exists.[59] These intersections of intersections could be anticipated using the cross product of the two vectors that define the $g-h$ plane.[126,127] Very recently we uncovered an interesting extension of this occurrence.[128,129] As noted previously in the tetra-atomic molecule HNCO, the ground $^1A'$ state and excited $^1A''$ state are connected by a symmetry-allowed seam of conical intersection for planar C_s geometries. For nonplanar geometries a seam of conical intersection of two states of the same symmetry also exists. These represent distinct branches of a common seam. What is surprising is that these seams intersect for C_s geometries. At these intersections $h = ||\mathbf{h}^{IJ}||$ vanishes. It can be shown that at the confluence the two seams have a common $\mathbf{g}^{IJ}$ direction.[128] However, $\mathbf{h}^{IJ}$ of one seam corresponds to a seam direction of the other seam. Thus, the minimal description of this confluence involves three internal coordinates, only one of which makes a linear contribution to the energy difference at the confluence. It will be important to establish the prevalence of this feature and determine whether it has a clear dynamical signature.

B. Role of Conical Intersections in Nonadiabatic Processes Involving LtU Transitions. The $O(^3P) + H_2O \rightarrow OH + OH$ reaction is a nonadiabatic process involving, at least formally, two or more changes of electronic state. The near linear conical intersection in Figure 4 guided our demonstration[135] of barrierless collinear paths connecting reactants and products. In addition, the collinear paths, by enforcing $^3\Pi$ and $^3\Delta$ degeneracies can reduce the number of nonadiabatic transitions required to reach the products. The wave packet studies of section IV show that sufficiently tilted cones can provide favorable pathways for LtU transitions. The importance of conical

intersections in UtL transitions is well established. However, this is not the case for LtU transitions, which are much less well studied in polyatomic molecules. It will be important to assess the extent to which the pathways offered by conical intersections are actually involved in this class of nonadiabatic processes.

VI. The Future

The study of electronically nonadiabatic processes goes back approximately 70 years to the pioneering work of Rice[130,131] and of London.[132] According to the golden rule[130,131] nonadiabatic transitions are driven by a product of the density of states and a coupling matrix element. The size of the matrix element is expected to increase if an avoided intersection is replaced by a conical intersection. Thus, the recent realization that conical intersections of states of the same symmetry are not rare occurrences necessitates a reevaluation of the importance of these two contributions to the decay mechanism. This will require both experimental and theoretical work on small systems in the gas phase where increasingly accurate models can be introduced and validated. Transfer of this expertise to the liquid phase and to larger (biologically relevant) systems, where nonadiabatic processes, have long been known and studied, has already begun and its continuation is essential. For adiabatic processes advanced tools for handling solvent effects are currently available,[133] as are techniques for handling larger systems by combining quantum mechanics and molecular mechanics.[134] The use of these techniques to address problems in nonadiabatic chemistry has already begun and can be expected to continue to grow in future.

Finally, we note that field of nonadiabatic dynamics has seen enormous growth with the advent of (efficient) algorithms for locating conical intersections in nonrelativistic Hamiltonians. These algorithms treat conical intersections of states of the same spin multiplicity but are otherwise quite general. (Algorithms for locating intersections of noninteracting states are not at issue here.) Very recently, an algorithm to locate conical intersections for Hamiltonians that include relativistic, spin−orbit, effects has been reported.[100] Such algorithms can be expected to bring similar insights to nonadiabatic processes for which relativistic effects are important.

In summary, nonadiabatic chemistry is a field with a long history and much work that remains to be done.

Appendix

The goal of this Appendix is to show how the deviations from a Jahn−Teller symmetric potential that occur for same-symmetry conical intersections are reflected in the Hamiltonian.

The wave packet Ψ^{T} is expanded in adiabatic electronic state basis

$$\Psi^{\mathrm{a,T}}(\mathbf{r},x,y,t) = \sum_{\alpha,K=I,J} \tilde{\Psi}^{\mathrm{a}}_{K}(\mathbf{r};x,y)\, \chi^{\mathrm{a},K}_{\alpha}(x,y)\, w^{\mathrm{a},K}_{\alpha}(t) \quad \text{(A1)}$$

The total Hamiltonian is given by[88]

$$\mathbf{H}^{\mathrm{T}}(x,y) = (2\mu)^{-1}\left[\begin{bmatrix} T^{+,II}(x,y) & k^{IJ}_{+}(x,y) \\ k^{IJ}_{+}(x,y) & T^{+,JJ}(x,y) \end{bmatrix} + T^{+,IJ}(x,y)\boldsymbol{\sigma}_y\right] + S(x,y)\mathbf{I} - \rho d_{gh} q(\phi)\boldsymbol{\sigma}_z \quad \text{(A2)}$$

where $q(\phi)^2 = (g^2 \cos^2\phi + h^2 \sin^2\phi)$

$$T^{+,KK}(x,y) = \mathbf{p}\cdot\mathbf{p} + (\mathbf{p}\cdot\nabla\mathbf{A}^K) + 2\nabla\mathbf{A}^K\cdot\mathbf{p} + \nabla\mathbf{A}^K\cdot\nabla\mathbf{A}^K + k^{KK} \quad \text{(A3a)}$$

$$T^{+,KL}(x,y) = (\mathbf{p} + \nabla\mathbf{A}^K)\cdot(-\mathrm{i})\bar{\mathbf{f}}^{K,L} + (-\mathrm{i})\bar{\mathbf{f}}^{L,K}\cdot(\mathbf{p} + \nabla\mathbf{A}^L) \quad \text{(A3b)}$$

where $k^{IJ} = \langle \mathbf{p}\Psi^{\mathrm{a}}_I | \cdot \mathbf{p}\Psi^{\mathrm{a}}_J\rangle$. In the symmetry-required case $q(\phi) = 1$, that is $g = h$. This can be formally achieved for this general case by the change of variables $x' = xg$, $y' = yh$. However, now the kinetic energy must be modified with $^1/_2\mathbf{p}\cdot\mathbf{p}$ replaced by $^1/_4\delta_{gh}{}^2(\mathbf{p}'\cdot\mathbf{p}' + \Delta_{gh}\mathbf{p}'\circ\mathbf{p}')$ where $\mathrm{A}\circ\mathrm{B} = \mathrm{A}_x\mathrm{B}_x - \mathrm{A}_y\mathrm{B}_y$. $\mathbf{H}^{\mathrm{T}}$ can be rewritten (dropping the primes), as

$$\mathbf{H}^{\mathrm{T}}(x,y) = \mathbf{H}^{\mathrm{sr}}(x,y) + \mathbf{K}^{\Delta}(x,y) + \mathbf{S}(x,y) \quad \text{(A4)}$$

where

$$\begin{aligned}\mathbf{H}^{\mathrm{sr},KL}(\mathrm{x},y) &= (2M)^{-1}\mathbf{T}^{+,KK}(x,y)\delta_{K,L} - \\ &\quad \rho d_{gh}\sigma_z^{KL} + (2M)^{-1}\mathbf{T}^{+,KL}(x,y)\sigma_{y,KL} \\ &\equiv H^{0,KK}(x,y) + T^{+,KL}(x,y)\end{aligned} \quad \text{(A5a)}$$

$$\mathbf{K}^{\Delta,KL}(x,y) = \mathbf{T}^{-,KK}(x,y)\delta_{K,L} + \mathbf{T}^{-,KL}(x,y)\sigma_{x,KL} \quad \text{(A5b)}$$

$$\mathbf{S}^{KL}(x,y) = S(x,y)\delta_{K,L} \quad \text{(A5c)}$$

where $\boldsymbol{T}^{-}$, eq A5b, is obtained from $\mathbf{T}^{+}$ by replacing $\cdot$ everywhere by $\circ$. Equation 4 is a principal result of this Appendix.

To take advantage of the fact that only the ϕ-component of the derivative coupling is singular, it is convenient to re-express eq 4 in polar coordinates. To this end, we replace

$$\chi^{\mathrm{a},I}_{\alpha} \rightarrow \chi_{Im\nu}(\rho,\phi) = \mathrm{e}^{\mathrm{i}m\phi}/\sqrt{(2\pi)}\rho^{-1/2}\xi^{I}_{m\nu}(\rho) \quad \text{(A6)}$$

and observe that $A^I = (l + {}^1/_2)\phi$, for l an integer; the singular component of the first derivaitve coupling $\rho^{-1}f^{IJ}_{\phi} = 1/(2\rho)$, and $\langle \mathbf{p}\Psi^{\mathrm{a}}_K | \cdot \mathbf{p}\Psi^{\mathrm{a}}_L\rangle = \rho^{-2}k^{KL}_{\phi} = \delta_{KL}\rho^{-2}f^{IJ}_{\phi}{}^2$, $\langle \mathbf{p}\Psi^{\mathrm{a}}_K | \circ \mathbf{p}\Psi^{\mathrm{a}}_L\rangle = k^{KL}_{-} = \delta_{KL}f^{IJ}_{\phi}\rho^{-2}\cos 2\phi$. Equation 5a becomes

$$T^{+,KK}_{n\nu,m\mu} = \delta_{mn}\left\langle \xi^{K}_{m\nu}\left| -\frac{\partial^2}{\partial\rho^2} + \frac{(l + m + {}^1/_2)^2}{\rho^2}\right|\xi^{K}_{m\mu}\right\rangle \quad \text{(A7a)}$$

$$T^{+,IJ}_{n\nu,m\mu} = -\mathrm{i}\delta_{m,n}\left\langle \xi^{I}_{m\nu}\left|\left(\frac{(m + l + {}^1/_2)}{\rho^2}\right)\right|\xi^{J}_{m\mu}\right\rangle \quad \text{(A7b)}$$

eq A5b becomes

$$\begin{aligned}K^{\Delta,KK}_{n\nu,m\mu} = \Bigg\langle \xi^{K}_{n\nu}\Bigg|\Bigg(&\frac{\delta_{n,m+2}}{2}\left[\frac{\partial^{\dagger}}{\partial\rho}\frac{\partial}{\partial\rho} - \frac{(m + l + 2)^2 - {}^5/_4}{\rho^2} + \frac{2(m + l + {}^3/_2)}{\rho}\frac{\partial}{\partial\rho}\right] + \\ &\frac{\delta_{n,m-2}}{2}\left[\frac{\partial^{\dagger}}{\partial\rho}\frac{\partial}{\partial\rho} - \frac{(m + l - 1)^2 - {}^5/_4}{\rho^2} - \frac{2(m + l - {}^1/_2)}{\rho}\frac{\partial}{\partial\rho}\right]\Bigg)\Bigg|\xi^{K}_{m\mu}\Bigg\rangle\end{aligned} \quad \text{(A8a)}$$

$$K^{\Delta,IJ}_{n\nu,m\mu} = iK^{\Delta,R,IJ}_{n\nu,m\mu} = \frac{i}{2}\left\langle \xi^I_{n\nu}\left|\left(\delta_{n,m+2}\left(\frac{(l+m+2)}{\rho^2} - \frac{1}{\rho}\frac{\partial}{\partial\rho}\right) + \delta_{n,m-2}\left(\frac{(l+m-1)}{\rho^2} + \frac{1}{\rho}\frac{\partial}{\partial\rho}\right)\right)\right|\xi^J_{m\mu}\right\rangle \quad \text{(A8b)}$$

and eq A5c becomes

$$S^{KL}_{n\nu,m\mu} = \delta_{KL}(\delta_{n,m+1}(s_x + is_y)/2 + \delta_{n,m-1}(s_x - is_y)/2)\langle\xi^K_{n\nu}|\rho|\xi^L_{m\mu}\rangle \quad \text{(A8c)}$$

Acknowledgment. This work was supported by the AFOSR, DoE Office of Basic Energy Sciences, and the National Science Foundation.

References and Notes

(1) Hu, X.; Schulten, K. *Phys. Today* **1997**, *50*, 28−34.
(2) Weber, W.; Helms, V.; McMCammon, A.; Langhoff, P. W. *Proc. Natl. Acad. Sci. U.S.A* **1999**, *96*, 6177−6182.
(3) *State-Selected and State-to-State Ion−Molecule Reaction Dynamics*; Baer, M., Ng, C.-Y., Eds.; John Wiley and Sons: New York, 1991; Parts 1 and 2, Vol. 82.
(4) Manthe, U.; Köppel, H. *J. Chem. Phys.* **1990**, *93*, 345.
(5) Manthe, U.; Köppel, H. *J. Chem. Phys.* **1990**, *93*, 1658.
(6) Müller, H.; Köppel, H. *Chem. Phys.* **1994**, *183*, 107−116.
(7) Baer, R.; Charutz, D. M.; Kosloff, R.; Baer, M. *J. Chem. Phys.* **1996**, *105*, 9141−9152.
(8) Baer, M. *J. Chem. Phys*. **1997**, *107*, 10662−10666.
(9) Baer, M.; Englman, R. *Chem. Phys. Lett* **1997**, *265*, 105−108.
(10) BenNun, M.; Martinez, T. D.; Levine, R. D. *Chem. Phys. Lett* **1997**, *270*, 319−326.
(11) Cattaneo, P.; Persico, M. *J. Phys. Chem. A* **1997**, *101*, 3454−3460.
(12) Ferretti, A.; Lami, A.; Villani, G. *J. Chem. Phys.* **1997**, *106*, 934.
(13) Martinez, T. J. *Chem. Phys. Lett* **1997**, *272*, 139−147.
(14) Klein, S.; Bearpark, M. J.; R.Smith, B.; Robb, M. A.; Olivucci, M.; Bernardi, F. *Chem. Phys. Lett.* **1998**, *292*, 259.
(15) Köppel, H.; Domcke, W. Vibronic Dynamics of Polyatomic Molecules. In *Encyclopedia of Computational Chemistry*; Schleyer, P. v. R., Ed.; Wiley: London, 1998.
(16) Adhikari, S.; Billing, G. D. *J. Chem. Phys* **1999**, *111*, 40−47.
(17) Ferretti, A.; Lami, A.; Villani, G. *J. Chem. Phys.* **1999**, *111*, 916−922.
(18) Mahapatra, S.; Köppel, H.; Cederbaum, L. S. *J. Chem. Phys* **1999**, *110*, 5691.
(19) Santoro, F.; Petrongolo, C. *J. Chem. Phys.* **1999**, *110*, 4419.
(20) Varandas, A. J. C.; Hu, H. G.; Xu, Z. R. *Mol. Phys.* **1999**, *96*, 1193.
(21) Varandas, A. J. C.; Xu, Z. R. *Chem. Phys. Lett* **2000**, *316*, 248−256.
(22) Varandas, A. J. C.; Xu, Z. R. *J. Chem. Phys.* **2000**, *1112*, 2121−2127.
(23) Michl, J.; Bonacic-Koutecky, V. *Electronic aspects of organic photochemistry*; Wiley: New York, 1990.
(24) Bernardi, F.; Olivucci, M.; Ragazos, I. N.; Robb, M. A. *J. Am. Chem. Soc.* **1992**, *114*, 2752.
(25) Domcke, W.; Stock, G. Theory of Ultrafast excited-state Nonadiabatic processes and their spectroscopic detection in real time. In *Advances in Chemistry and Physics*; Prigogine, I., Rice, S. A., Eds.; J. Wiley: New York, 1997; Vol. 100, pp 1−168.
(26) Fuss, W.; Lochbrunner, S.; Müller, A. M.; Schikarski, T.; Schmid, W. E.; Trushi, S. A. *Chem. Phys.* **1998**, *232*, 161−174.
(27) Mahapatra, S.; Köppel, H. *J. Chem. Phys* **1998**, *109*, 1721−1733.
(28) Mahapatra, S.; Köppel, H. *Phys. Rev. Lett* **1998**, *81*, 3116−3119.
(29) Trushin, S. A.; Fuss, W.; Schmid, W. E.; Kompa, K. L. *J. Phys. Chem. A* **1998**, *102*, 4129−4137.
(30) Diau, E. W.-G.; Feyter, S. D.; Zewail, A. H. *J. Chem. Phys.* **1999**, *110*, 9785−9788.
(31) Krawczyk, R. P.; Malsch, K.; Hohlneciher, G.; Gillen, R. C.; Domke, W. *Chem. Phys. Lett* **2000**, *320*, 535−541.
(32) Atchity, G. J.; Xantheas, S. S.; Ruedenberg, K. *J. Chem. Phys.* **1991**, *95*, 1862.
(33) Yarkony, D. R. *J. Chem. Phys.* **2001**, *114*, 2601−2613.
(34) *State-Selected and State-to-State Ion−Molecule Reaction Dynamics: Part 2 Theory*; Baer, M., Ng, C.-Y., Eds.; J. Wiley and Sons: New York, 1992; Vol. 82.
(35) Bernardi, F.; Olivucci, M.; Ragazos, I. N.; Robb, M. A. *J. Am. Chem. Soc.* **1992**, *114*, 8211.
(36) Hoffman, B. C.; Yarkony, D. R. *J. Chem. Phys.* **2000**, *113*, 10091−10099.
(37) Longuet-Higgins, H. C. *Adv. Spectrosc.* **1961**, *2*, 429−472.
(38) Mead, C. A. *J. Chem. Phys.* **1983**, *78*, 807−814.
(39) Berry, M. V. *Proc. R. Soc. London Ser. A* **1984**, *392*, 45−57.
(40) Born, M.; Oppenheimer, J. R. *Ann. Phys. (Leipzig)* **1927**, *84*, 457.
(41) Yarkony, D. R. *Acc. Chem. Res.* **1998**, *31*, 511−518.
(42) Mead, C. A.; Truhlar, D. G. *J. Chem. Phys.* **1979**, *70*, 2284−2296.
(43) von Neumann, J.; Wigner, E. *Phys. Z.* **1929**, *30*, 467−470.
(44) Lengsfield, B. H.; Yarkony, D. R. Nonadiabatic Interactions Between Potential Energy Surfaces: Theory and Applications. In *State-Selected and State to State Ion−Molecule Reaction Dynamics: Part 2 Theory*; Baer, M., Ng, C.-Y., Eds.; John Wiley and Sons: New York, 1992; Vol. 82, pp 1−71.
(45) Baer, M. *Chem. Phys. Lett.* **1975**, *35*, 112−118.
(46) Pacher, T.; Cederbaum, L. S.; Köppel, H. *Adv. Chem. Phys.* **1993**, *84*, 293−391.
(47) Yarkony, D. R. *J. Phys. Chem. A* **1997**, *101*, 4263−4270.
(48) Kuppermann, A. The Geometric Phase in Reaction Dynamics. In *Dynamics of Molecules and Chemical reactions*; Wyatt, R. E., Zhang, J. Z. H., Eds.; Marcel Dekker: New York, 1996; pp 411−472.
(49) (a) Molnar, F.; Ben-Nun, M.; Martinez, T. J.; Chulten, K. S. *J. Mol. Struct. (THEOCHEM.)* **2000**, *506*, 169−178. (b) Logunov, S. L.; Song, L.; El-Sayed, M. A. *J. Phys. Chem*. **1996**, *100*, 18586−18591.
(50) Kim, S. K.; Lovejoy, E. R.; Moore, C. B. *Science* **1992**, *256*, 1541.
(51) Yarkony, D. R. *J. Phys. Chem. A* **1999**, *103*, 6658−6668.
(52) Mead, C. A. *J. Chem. Phys.* **1980**, *72*, 3839.
(53) Fang, W.-H.;.You, X.-Z.; Yin, Z. *Chem. Phys. Lett* **1995**, *238*, 236.
(54) Mebel, A.; Luna, A.; Lin, M. C.; Morokuma, K. *J. Chem. Phys.* **1996**, *105*, 6439.
(55) Stevens, J. E.; Cui, Q.; Morokuma, K. *J. Chem. Phys.* **1998**, *108*, 1452−1458.
(56) Kaledin, A. L.; Cui, Q.; Heaven, M. C.; Morokuma, K. *J. Chem. Phys.* **1999**, *111*, 5004−5016.
(57) Klossika, J. J.; Flöthmann, H.; Schinke, R.; Bitterерova, M. *Chem. Phys. Lett.* **1999**, *314*, 183−188.
(58) Klossika, J. J.; Schinke, R. *J. Chem. Phys.* **1999**, *111*, 5882.
(59) Yarkony, D. R. *J. Chem. Phys.* **2001**, *114*, 2614.
(60) Gimelshein, S. F.; Levin, D. A. Modeling of OH Vibrational Distributions Using Molecular Dynamics with the Direct Simulation Monte Carlo Method. 34th Theromophysics Conferences, 2000, Denver CO.
(61) Gimelshein, S. F.; Levin, D. A.; Drakes, J. A.; Karabadzhak, G. F.; Plastinin, Y. DSMC Modeling of Chemically Reacting two- and three-dimensional flows from Soyuz-TM Rocket Exhaust Plumes. 34th Thermophysics Conferences, 2000, Denver CO.
(62) Gimelshein, S. F.; Levin, D. A.; Drakes, J. A.; Karabadzhak, G. F.; Ivanov, M. S. *AIAA* **2001**, *131*, 100.
(63) Yarkony, D. R. *Mol. Phys.* **1998**, *93*, 971−983.
(64) Dixon, R. N.; Huang, D. W.; Yang, X. F.; Harich, S.; Lin, J. J.; Yang, X. *Science* **1999**, *285*, 1249−1253.
(65) Köppel, H.; Domcke, W.; Cederbaum, L. S. *Adv. Chem. Phys.* **1984**, *57*, 59.
(66) Naqvi, K. R. *Chem. Phys. Lett* **1972**, *15*, 634.
(67) Naqvi, K. R.; Byers Brown, W. *Int. J. Quantum Chem.* **1972**, *6*, 271.
(68) Yarkony, D. R. Electronic Structure Aspects of Nonadiabatic Processes in Polyatomic Systems. In *Modern Electronic Structure Theory*; Yarkony, D. R., Ed.; World Scientific: Singapore, 1995; pp 642−721.
(69) Lefebvre-Brion, H.; Field, R. W. *Perturbations in the Spectra of Diatomic Molecules*; Academic Press: New York, 1986.
(70) Smith, F. T. *Phys. Rev.* **1969**, *179*, 111−123.
(71) Sidis, V. Diabatic Potential Energy Surfaces for Charge-Transfer Processes. In *State-Selected and State-to-State Ion−Molecule Reaction Dynamics Part 2, Theory*; Baer, M., Ng, C.-Y., Eds.; John Wiley and Sons: New York, 1992; Vol. 82, pp 73−134.
(72) Lichten, W. *Phys. Rev.* **1963**, *131*, 229−238.
(73) O'Malley, T. F. In *Advances in Atomic and Molecular Physics*; Bates, D. R., Esterman, I., Eds.; Academic: New York, 1971; Vol. 7, pp 223−249.
(74) Mead, C. A.; Truhlar, D. G. *J. Chem. Phys.* **1982**, *77*, 6090−6098.
(75) Thiel, A.; Köppel, H. *J. Chem. Phys.* **1999**, *110*, 9371−9382.
(76) Werner, H. J.; Meyer, W. *J. Chem. Phys.* **1981**, *74*, 5802−5807.
(77) Atchity, G. J.; Ruedenberg, K. *Theor. Chem. Acc.* **1997**, *97*, 47−58.
(78) Kryachko, E. S.; Yarkony, D. R. *Int. J. Quantum Chem.* **2000**, *76*, 235−243.
(79) Englman, R. *The Jahn−Teller Effect in Molecules and Crystals*; Wiley-Interscience: New York, 1972.
(80) Bersuker, I. B. *The Jahn−Teller Effect and Vibronic Interactions in Modern Chemistry*; Plenum: New York, 1984.
(81) Langhoff, S. R.; Kern, C. W. Molecular Fine Structure. In *Modern Theoretical Chemistry*; Schaefer, H. F., Ed.; Plenum: New York, 1977; Vol. 4, p 381.

(82) Yarkony, D. R. *Int. Rev. Phys. Chem.* **1992**, *11*, 195−242.
(83) Kramers, H. *Proc. Acad. Sci. Amsterdam* **1930**, *33*, 959.
(84) Schiff, L. I. *Quantum Mechanics*; McGraw-Hill: New York, 1960.
(85) Mead, C. A. *Chem. Phys.* **1980**, *49*, 33−38.
(86) Kuppermann, A.; Wu, Y.-S. M. *Chem. Phys. Lett.* **1993**, *205*, 577.
(87) Berry, M. V.; Wilkinson, M. *Proc. R. Soc. (London), Ser. A* **1984**, *392*, 15−43.
(88) Yarkony, D. R. *Rev. Mod. Phys.* **1996**, *68*, 985−1013.
(89) Varandas, A. J. C.; Tennyson, J.; Mjurrell, J. N. *Chem. Phys. Lett.* **1979**, *61*, 431.
(90) Xantheas, S.; Elbert, S. T.; Ruedenberg, K. *J. Chem. Phys.* **1990**, *93*, 7519−7521.
(91) Yarkony, D. R. *J. Chem. Phys.* **1996**, *104*, 2932−2939.
(92) Baer, M. *Mol. Phys.* **1980**, *40*, 1011−1013.
(93) Glezakou, V.-A.; Gordon, M. S.; Yarkony, D. R. *J. Chem. Phys* **1998**, *108*, 5657−5659.
(94) Matsunaga, N.; Yarkony, D. R. *Mol. Phys.* **1998**, *93*, 79−84.
(95) Yarkony, D. R. *J. Chem. Phys.* **1999**, *111*, 6661−6664.
(96) Mebel, A.; Baer, M.; Lin, S. H. *J. Chem. Phys.* **2000**, *112*, 10703−10706.
(97) Stone, A. J. *Proc. R. Soc. London A* **1976**, *351*, 141−150.
(98) R.Englman; Baer, M. *J. Phys.: Condens. Matter* **1999**, *11*, 1059−1067.
(99) Bethe, H. A.; Salpeter, E. E. *Quantum Mechanics of One and Two Electron Atoms*; Plenum/Rosetta: New York, 1977.
(100) Matsika, S.; Yarkony, D. R. *J. Chem. Phys.*, in press.
(101) Yarkony, D. R. *J. Phys. Chem.* **1996**, *100*, 18612−18628.
(102) Yamaguchi, Y.; Osamura, Y.; Goddard, J. D.; Schaefer, H. F. *A New Dimension to Quantum Chemistry: Analytic Derivative Methods in ab initio Molecular Electronic Structure Theory*; Oxford University Press: Oxford, U.K., 1994.
(103) Shepard, R. The Analytic Gradient Method for Configuartion Interaction Wave functions. In *Modern Electronic Structure Theory*; Yarkony, D. R., Ed.; World Scientific Publishing: Singapore, 1995; Vol. 2, pp 345−458.
(104) Yarkony, D. R. Molecular Structure. In *Atomic, Molecular and Optical Physics Handbook*; Drake, G. L., Ed.; AIP: New York, 1996; pp 357−377.
(105) Yarkony, D. R. *J. Chem. Phys.* **2000**, *112*, 2111−2120.
(106) Carrington, T. *Acc. Chem. Res.* **1974**, *7*, 20−25.
(107) *Quantum Chemistry. Classic Scientific Papers*; Hettema, H., Ed.; World Scientific: Singapore, 2000.
(108) Mead, C. A. *J. Chem. Phys.* **1979**, *70*, 2276.
(109) Bearpark, M. J.; Robb, M. A.; Schlegel, H. B. *Chem. Phys. Lett.* **1994**, *223*, 269−274.
(110) Yarkony, D. R. *J. Phys. Chem. A* **1998**, *102*, 8073−8077.
(111) Top, Z.; Baer, M. *Chem. Phys.* **1977**, *25*, 1.
(112) Tinkham, M. *Group Theory and Quantum Mechanics*; McGraw-Hill: New York, 1964.
(113) Yarkony, D. R. *J. Chem. Phys.* **1988**, *89*, 7324−7333.
(114) Chaban, G.; Gordon, M. S. *Chem. Phys. Lett.* **1997**, *278*, 195−201.
(115) Williams, J.; Alexander, M. H. *J. Chem. Phys.* **2000**, *112*, 5722−5730.
(116) Lester, M. I.; Loomis, R. A.; Schwartz, R. L.; Walch, S. P. *J. Phys. Chem. A* **1997**, *101*, 9195−9206.
(117) Loomis, R. A.; Lester, M. I. *Annu. Rev. Phys. Chem.* **1997**, *48*, 643−673.
(118) Herzberg, G.; Longuet-Higgins, H. C. *Discuss. Faraday Soc.* **1963**, *35*, 77.
(119) Schön, J.; Köppel, H. *J. Chem. Phys.* **1998**, *108*, 1503−1513.
(120) Kendrick, B. *Phys. Rev. Lett.* **1997**, *79*, 2431−2433.
(121) Kendrick, B. K.; Mead, C. A.; Truhlar, D. G. *J. Chem. Phys.* **1999**, *107*, 7594−7597.
(122) Kuntz, P. J.; Whitton, W. N.; Paidarova, I.; Polak, R. *Can. J. Chem.* **1994**, *72*, 939.
(123) Atchity, G. J.; Ruedenberg, K.; Nanayakkara, A. *Theor. Chem. Acc.* **1997**, *96*, 195−204.
(124) Chaban, G.; Gordon, M. S.; Yarkony, D. R. *J. Phys. Chem. A* **1997**, *101*, 7953−7959.
(125) Matsunaga, N.; Yarkony, D. R. *J. Chem. Phys.* **1997**, *107*, 7825−7838.
(126) Yarkony, D. R. *Theor. Chem. Acc.* **1997**, *98*, 197−201.
(127) Yarkony, D. R. *J. Chem. Phys.* **1998**, *109*, 7047−7050.
(128) Yarkony, D. R. *J. Phys. Chem. A* **2001**, *103*, 2642−2645.
(129) Yarkony, D. R. *Mol. Phys.*, in press.
(130) Rice, O. K. *Phys. Rev.* **1929**, *33*, 748−759.
(131) Rice, O. K. *Phys. Rev.* **1929**, *34*, 1451−1462.
(132) London, F. *Z. Phys.* **1932**, *74*, 132.
(133) Bandyopadhyay, P.; Gordon, M. S. *J. Chem. Phys.* **2000**, *113*, 1104.
(134) Vrehen, T.; Morokuma, K. *J. Chem. Phys.* **2000**, *113*, 2969.
(135) Matsika, S.; Yarkony, D. R. Manuscript in preparation.